



UNIVERSITY OF HULL | FACULTY OF BUSINESS,  
LAW AND POLITICS

The Centre for Systems Studies presents



# How to Reveal Neuroblastoma's Emergent Properties at Different Biological Scales

Dr Kenneth Y. Wertheim, University of Hull

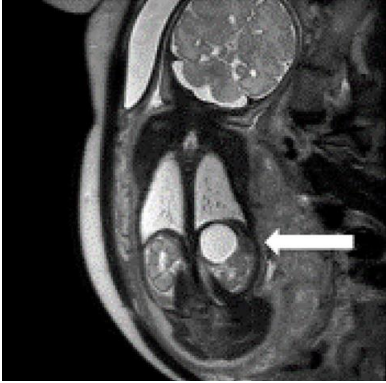
10 April 2024, 2-3.30pm (UK time)  
Derwent SR1-1A & Online

Dr Kenneth Y. Wertheim  
Also known as 11250205  
Pronouns: they/them  
[k.y.wertheim@hull.ac.uk](mailto:k.y.wertheim@hull.ac.uk)  
<https://kywertheim.com>

# Lecture outline

1. **Neuroblastoma.**
2. Multiscale problem.
3. Tumour scale.
4. Tissue scale.
5. Cellular scale.

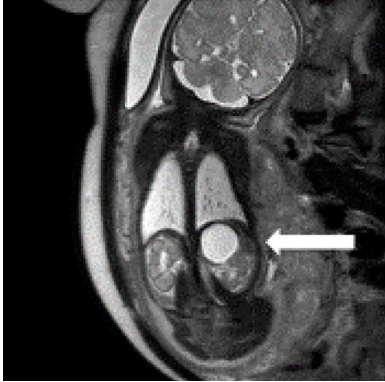
# Neuroblastoma



Louis, Chrystal U., and Jason M. Shohet.  
"Neuroblastoma: molecular pathogenesis and  
therapy." *Annual review of medicine* 66 (2015): 49.

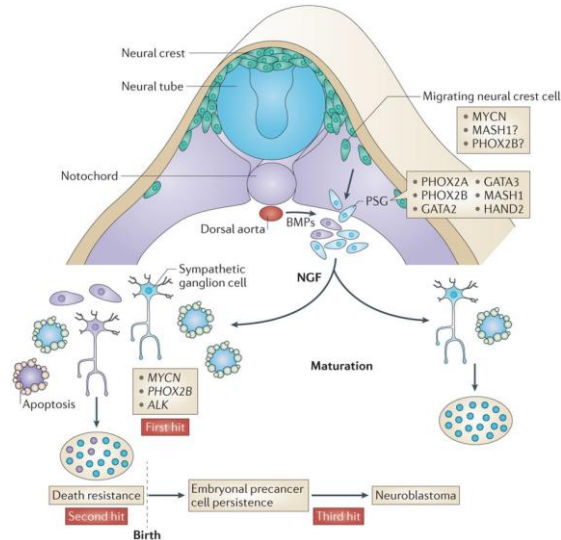
1. Adrenal medulla is the usual primary site.
2. Most common extracranial solid tumour in children.
3. 15 % of cancer-related deaths in this population.

# Neuroblastoma



Louis, Chrystal U., and Jason M. Shohet. "Neuroblastoma: molecular pathogenesis and therapy." *Annual review of medicine* 66 (2015): 49.

1. Adrenal medulla is the usual primary site.
2. Most common extracranial solid tumour in children.
3. 15 % of cancer-related deaths in this population.

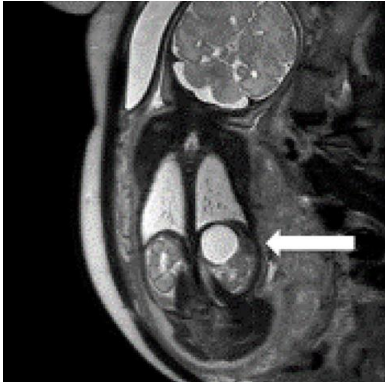


Nature Reviews | Cancer

Marshall, Glenn M., et al. "The prenatal origins of cancer." *Nature Reviews Cancer* 14.4 (2014): 277-289.

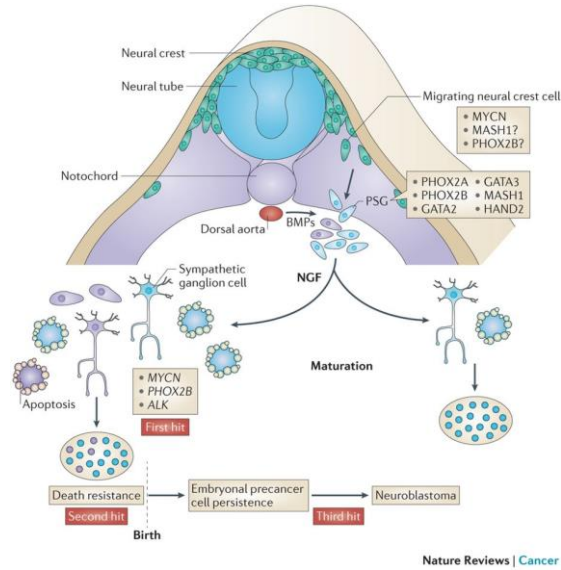
1. Neural crest, transient in the embryo.
2. Differentiate into different cell types.
3. Sympathetic nervous system.
4. MYCN amplification and ALK activation turn them into neuroblastoma cancer cells.

# Neuroblastoma



Louis, Chrystal U., and Jason M. Shohet. "Neuroblastoma: molecular pathogenesis and therapy." *Annual review of medicine* 66 (2015): 49.

1. Adrenal medulla is the usual primary site.
2. Most common extracranial solid tumour in children.
3. 15 % of cancer-related deaths in this population.



Nature Reviews | Cancer

Marshall, Glenn M., et al. "The prenatal origins of cancer." *Nature Reviews Cancer* 14.4 (2014): 277-289.

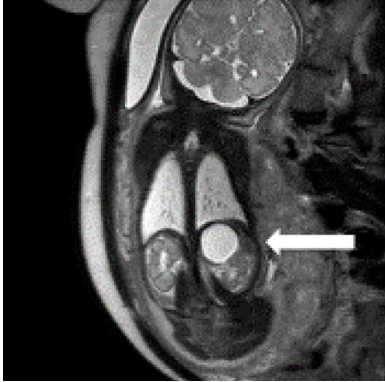
1. Neural crest, transient in the embryo.
2. Differentiate into different cell types.
3. Sympathetic nervous system.
4. MYCN amplification and ALK activation turn them into neuroblastoma cancer cells.

INRG Stage	Age (months)	Histologic Category	Grade of Tumor Differentiation	MYCN	11q Aberration	Ploidy	Pretreatment Risk Group	
L1/L2		GN maturing; GNB intermixed		NA			A Very low	
L1		Any, except GN maturing or GNB intermixed		NA			B Very low	
				Amp			K High	
L2	< 18	Any, except GN maturing or GNB intermixed	Differentiating	NA	No		D Low	
					Yes		G Intermediate	
	≥ 18		GNB nodular; neuroblastoma	Poorly differentiated or undifferentiated	NA	No		E Low
						Yes		H Intermediate
				Amp			N High	
M	< 18			NA		Hyperdiploid	F Low	
	< 12			NA		Diploid	I Intermediate	
	12 to < 18			NA		Diploid	J Intermediate	
	< 18			Amp			O High	
	≥ 18						P High	
MS	< 18			NA	No		C Very low	
					Yes		Q High	
					Amp		R High	

Sokol, Elizabeth, and Ami V. Desai. "The evolution of risk classification for neuroblastoma." *Children* 6.2 (2019): 27.

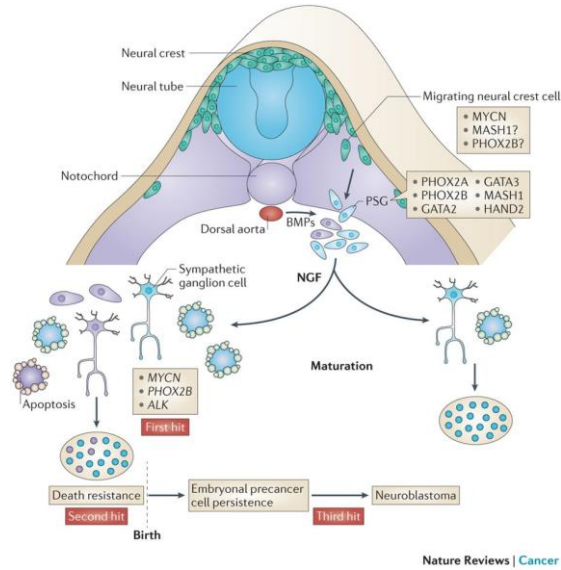
1. Low risk, spontaneous regression.

# Neuroblastoma



Louis, Chrystal U., and Jason M. Shohet. "Neuroblastoma: molecular pathogenesis and therapy." *Annual review of medicine* 66 (2015): 49.

1. Adrenal medulla is the usual primary site.
2. Most common extracranial solid tumour in children.
3. 15 % of cancer-related deaths in this population.



Marshall, Glenn M., et al. "The prenatal origins of cancer." *Nature Reviews Cancer* 14.4 (2014): 277-289.

1. Neural crest, transient in the embryo.
2. Differentiate into different cell types.
3. Sympathetic nervous system.
4. MYCN amplification and ALK activation turn them into neuroblastoma cancer cells.

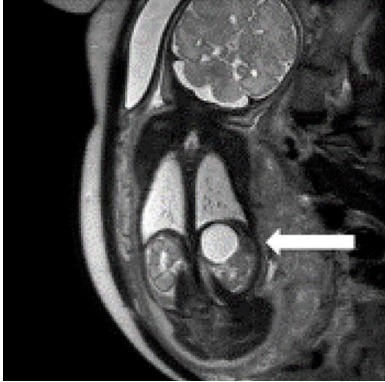
INRG Stage	Age (months)	Histologic Category	Grade of Tumor Differentiation	MYCN	11q Aberration	Ploidy	Pretreatment Risk Group
L1/L2		GN maturing; GNB intermixed		NA			A Very low
L1		Any, except GN maturing or GNB intermixed		NA			B Very low
				Amp			K High
L2	< 18	Any, except GN maturing or GNB intermixed	Differentiating	NA	No		D Low
				NA	Yes		G Intermediate
	≥ 18	GNB nodular; neuroblastoma	Poorly differentiated or undifferentiated	NA	No		E Low
				NA	Yes		H Intermediate
				Amp			N High
M	< 18			NA		Hyperdiploid	F Low
	< 12			NA		Diploid	I Intermediate
	12 to < 18			NA		Diploid	J Intermediate
	< 18			Amp			O High
	≥ 18						P High
MS	< 18			NA	No		C Very low
				NA	Yes		Q High
				Amp			R High

Sokol, Elizabeth, and Ami V. Desai. "The evolution of risk classification for neuroblastoma." *Children* 6.2 (2019): 27.

1. Low risk, spontaneous regression.
2. High risk, 50 % relapse.

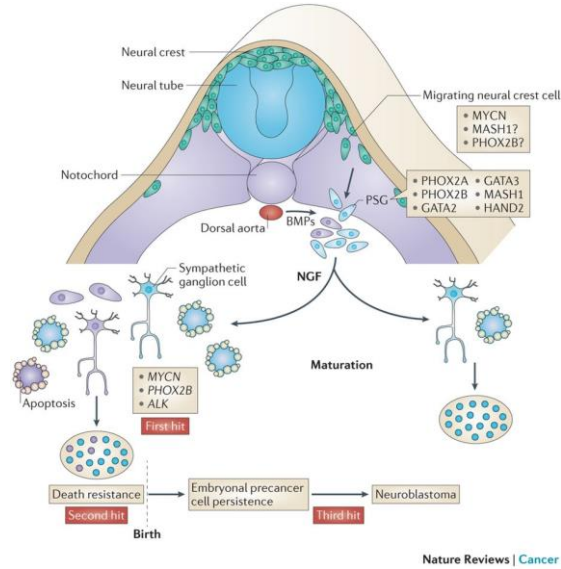


# Neuroblastoma



Louis, Chrystal U., and Jason M. Shohet. "Neuroblastoma: molecular pathogenesis and therapy." *Annual review of medicine* 66 (2015): 49.

1. Adrenal medulla is the usual primary site.
2. Most common extracranial solid tumour in children.
3. 15 % of cancer-related deaths in this population.



Nature Reviews | Cancer

Marshall, Glenn M., et al. "The prenatal origins of cancer." *Nature Reviews Cancer* 14.4 (2014): 277-289.

1. Neural crest, transient in the embryo.
2. Differentiate into different cell types.
3. Sympathetic nervous system.
4. MYCN amplification and ALK activation turn them into neuroblastoma cancer cells.

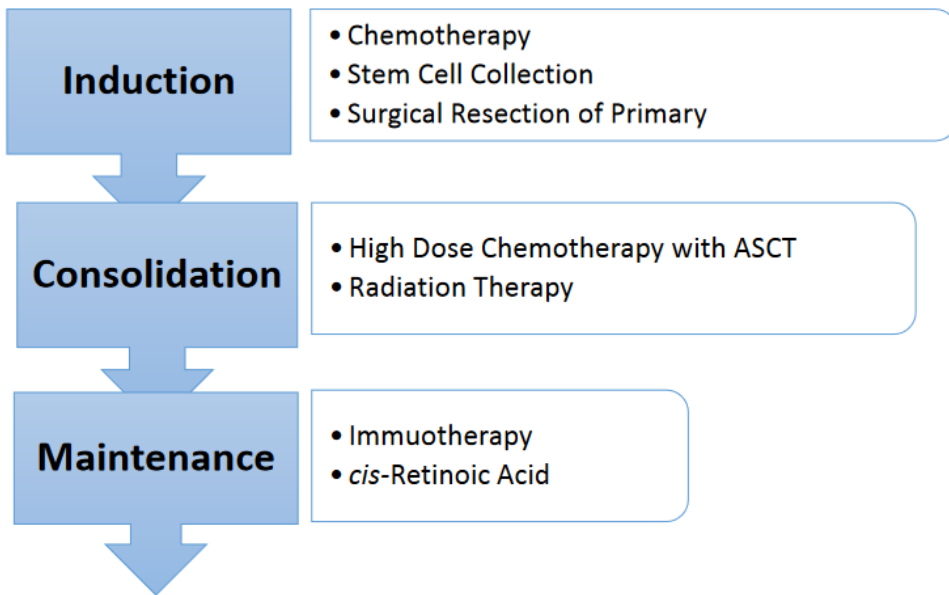
INRG Stage	Age (months)	Histologic Category	Grade of Tumor Differentiation	MYCN	11q Aberration	Ploidy	Pretreatment Risk Group
L1/L2		GN maturing; GNB intermixed		NA			A Very low
L1		Any, except GN maturing or GNB intermixed		NA			B Very low
				Amp			K High
L2	< 18	Any, except GN maturing or GNB intermixed	Differentiating	NA	No		D Low
				NA	Yes		G Intermediate
	≥ 18	GNB nodular; neuroblastoma	Poorly differentiated or undifferentiated	NA	No		E Low
				NA	Yes		H Intermediate
				Amp			N High
M	< 18			NA		Hyperdiploid	F Low
	< 12			NA		Diploid	I Intermediate
	12 to < 18			NA		Diploid	J Intermediate
	< 18			Amp			O High
	≥ 18						P High
MS	< 18			NA	No		C Very low
				NA	Yes		Q High
				Amp			R High

Sokol, Elizabeth, and Ami V. Desai. "The evolution of risk classification for neuroblastoma." *Children* 6.2 (2019): 27.

1. Low risk, spontaneous regression.
2. High risk, 50 % relapse.
3. MYCN amplification is a bad sign.

# Neuroblastoma

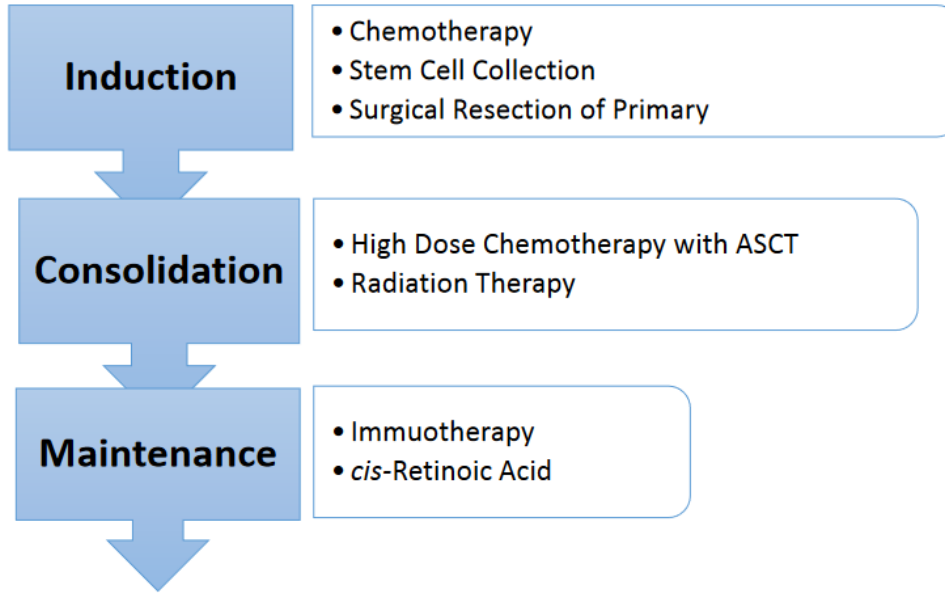
Current standard:  
multi-modal therapy.





# Neuroblastoma

Current standard:  
multi-modal therapy.



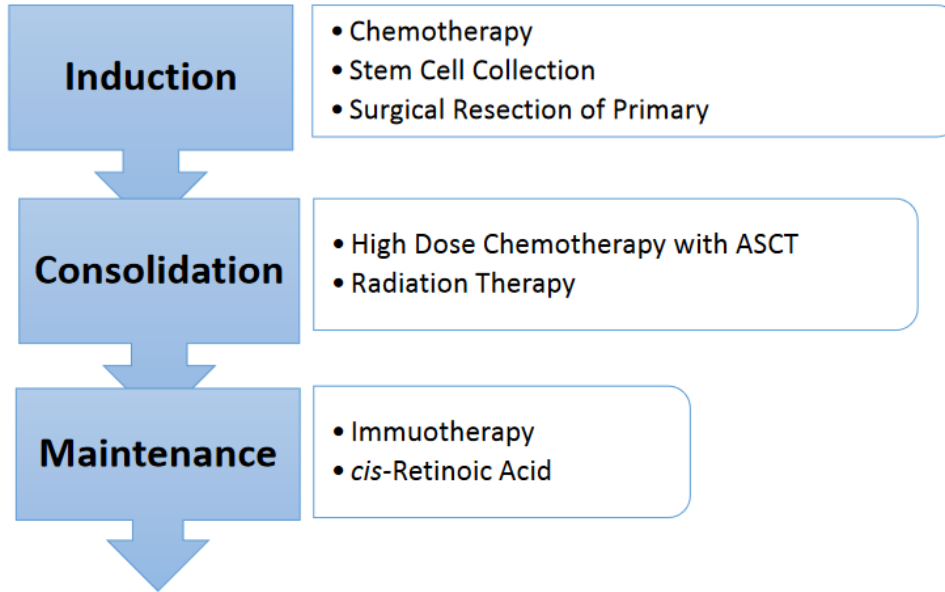
High risk, 50 % relapse.

Mutations can occur in the entire genome.

Effectively innumerable resistance strategies.

# Neuroblastoma

Current standard:  
multi-modal therapy.



Smith, Valeria, and Jennifer Foster. "High-risk neuroblastoma treatment review." *Children* 5.9 (2018): 114.

## Integrating evolutionary dynamics into cancer therapy

Robert A. Gatenby, [✉](#) & Joel S. Brown

*Nature Reviews Clinical Oncology* 17, 675–686 (2020) | [Cite this article](#)

7157 Accesses | 96 Citations | 271 Altmetric | [Metrics](#)

### Abstract

Many effective drugs for metastatic and/or advanced-stage cancers have been developed over the past decade, although the evolution of resistance remains the major barrier to disease control or cure. In large, diverse populations such as the cells that compose metastatic cancers, the emergence of cells that are resistant or that can quickly develop resistance is virtually inevitable and most likely cannot be prevented. However, clinically significant resistance occurs only when the pre-existing resistant phenotypes are able to proliferate extensively, a process governed by eco-evolutionary dynamics. Attempts to disrupt the molecular mechanisms of resistance have generally been unsuccessful in clinical practice. In this Review, we focus on the Darwinian processes driving the eco-evolutionary dynamics of treatment-resistant cancer populations. We describe a variety of evolutionarily informed strategies designed to increase the probability of disease control or cure by anticipating and steering the evolutionary dynamics of acquired resistance.

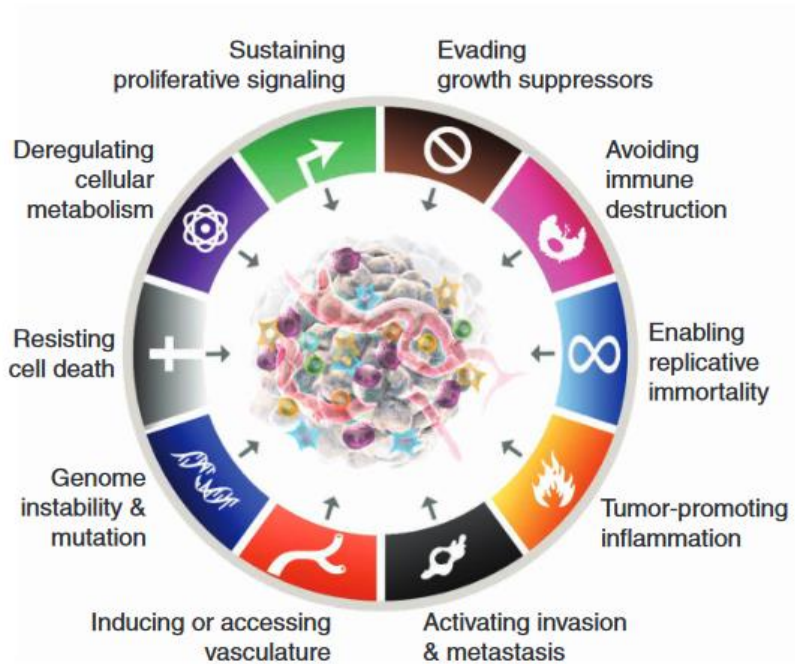
Gatenby, Robert A., and Joel S. Brown. "Integrating evolutionary dynamics into cancer therapy." *Nature reviews Clinical oncology* 17.11 (2020): 675-686.

## One-size-fits-all strategy ignores evolutionary dynamics.

# Lecture outline

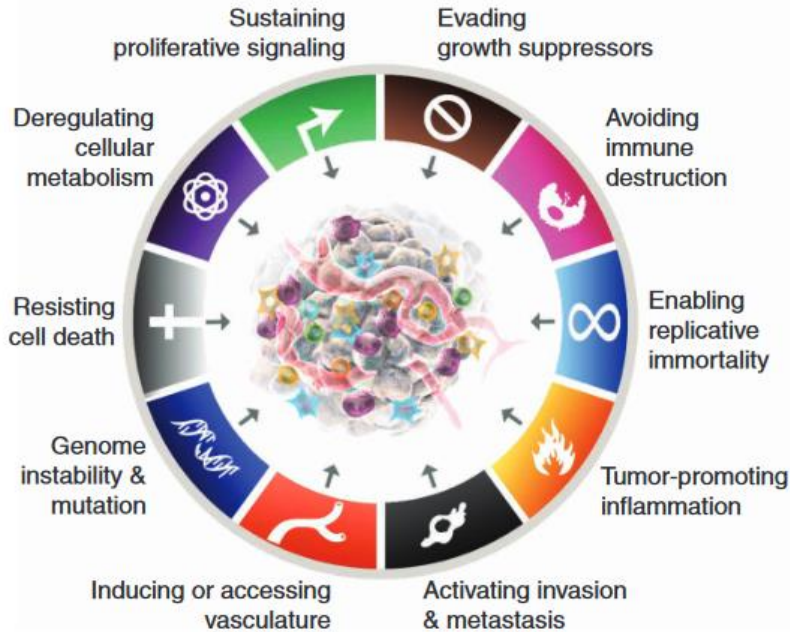
- ~~1. Neuroblastoma.~~
- 2. Multiscale problem.**
3. Tumour scale.
4. Tissue scale.
5. Cellular scale.

# Multiscale problem

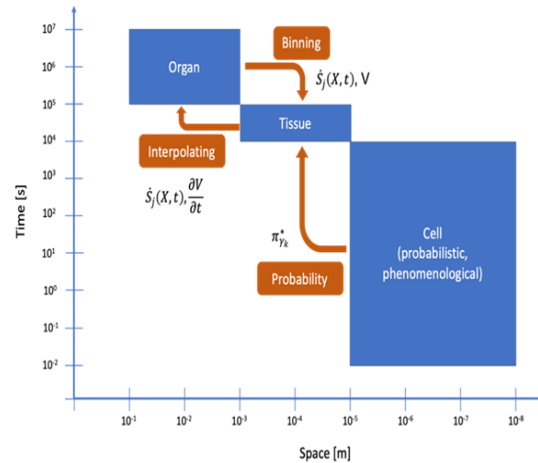


Hanahan, Douglas. "Hallmarks of cancer: new dimensions." *Cancer discovery* 12.1 (2022): 31-46.

# Multiscale problem



Hanahan, Douglas. "Hallmarks of cancer: new dimensions." *Cancer discovery* 12.1 (2022): 31-46.



de Melo Quintela, Bárbara, et al. "A theoretical analysis of the scale separation in a model to predict solid tumour growth." *Journal of Theoretical Biology* 547 (2022): 111173.

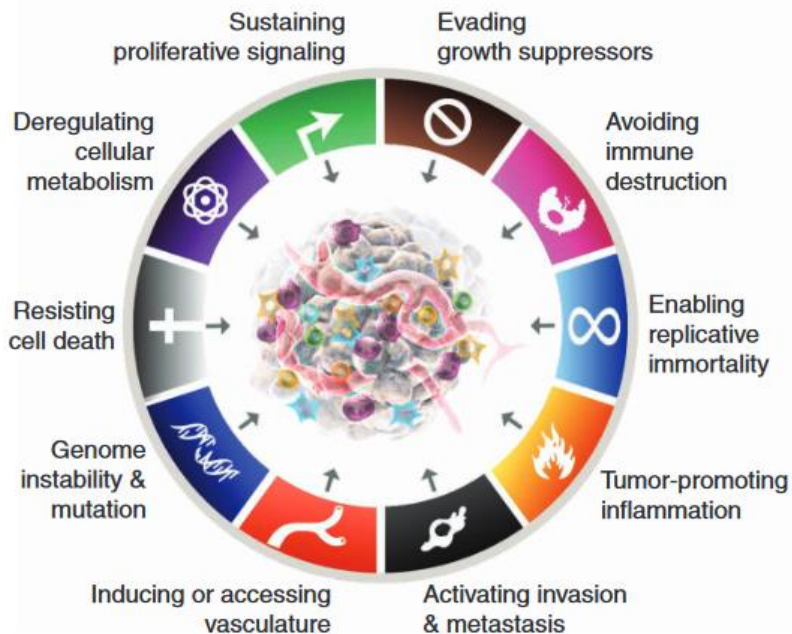


ALMA MATER STUDIORUM  
UNIVERSITÀ DI BOLOGNA

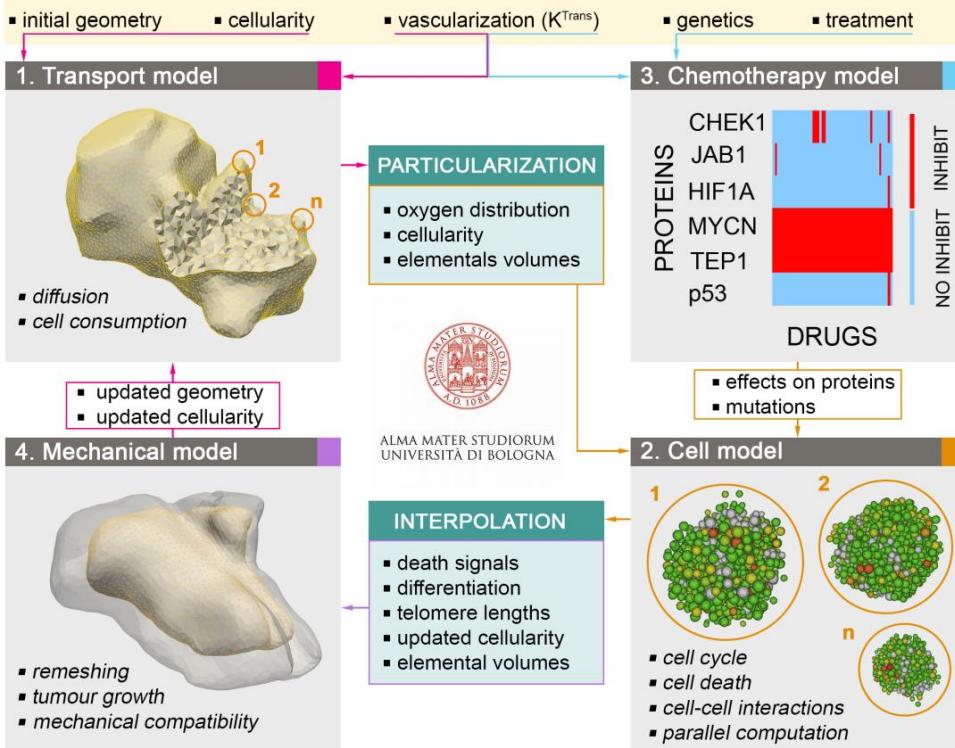
Cannot describe biological phenomena spanning **nine orders of magnitude** in a single-scale model.

- Experimental resolutions.
- Model complexity.
- Computational costs.

# Primage (2019–2022)



## PATIENT DATA

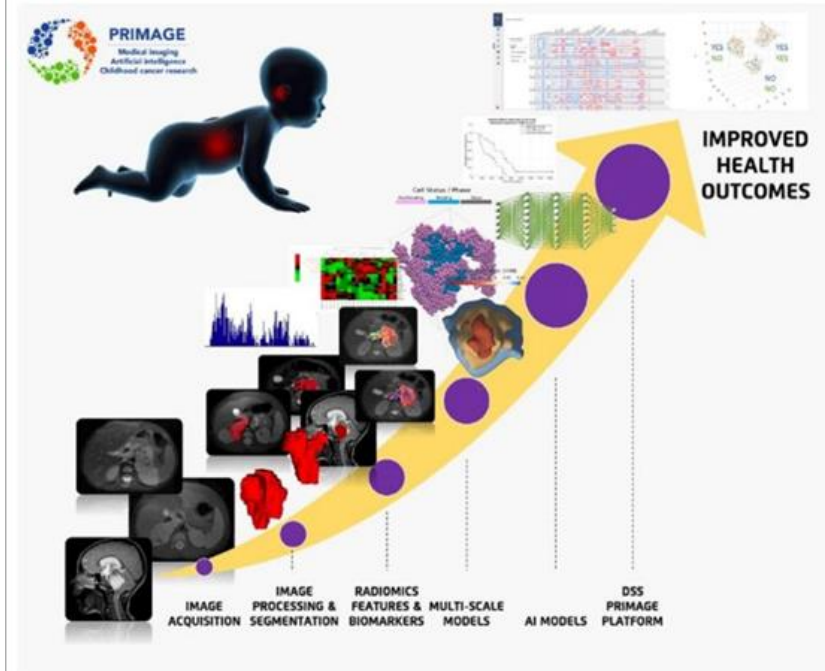


Hanahan, Douglas. "Hallmarks of cancer: new dimensions." *Cancer discovery* 12.1 (2022): 31-46.

Borau, Carlos, et al. "A multiscale orchestrated computational framework to reveal emergent phenomena in neuroblastoma." *Computer Methods and Programs in Biomedicine* 241 (2023): 107742.



# Primage (2019–2022)



Decision support system for the clinical management of malignant solid tumours.

1. Image acquisition, processing, and segmentation.
2. Integrate radiomic features with other biomarkers, such as mutations and histology.
3. **Multiscale models: organ/tumour, tissue, and intracellular.**
4. Machine learning techniques extract insights from simulation results.

# Lecture outline

~~1. Neuroblastoma.~~

~~2. Multiscale problem.~~

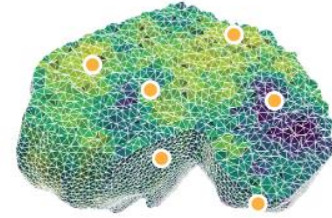
**3. Tumour scale.**

4. Tissue scale.

5. Cellular scale.

Population-based approach

Scale: Whole tumour.

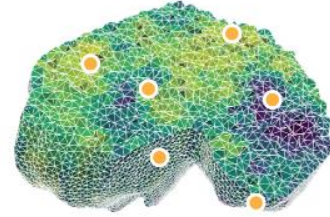


# Population-based approach

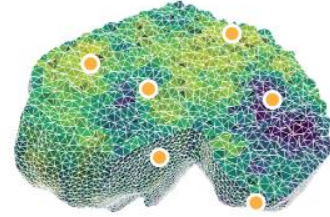
Scale: Whole tumour.

Resolution: Population containing identical cells.

A tumour is represented by multiple populations with a total size below a carrying capacity.



# Population-based approach



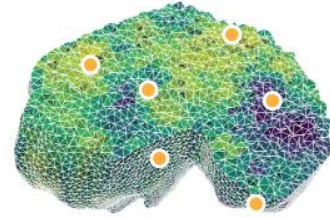
Scale: Whole tumour.

Resolution: Population containing identical cells.

A tumour is represented by multiple populations with a total size below a carrying capacity.

Modelling framework: Differential equations.

# Population-based approach



Scale: Whole tumour.

Resolution: Population containing identical cells.

A tumour is represented by multiple populations with a total size below a carrying capacity.

Modelling framework: Differential equations.

Cellular events are stochastic. Many cells, many events. Average over them.

1000000.7 cells.

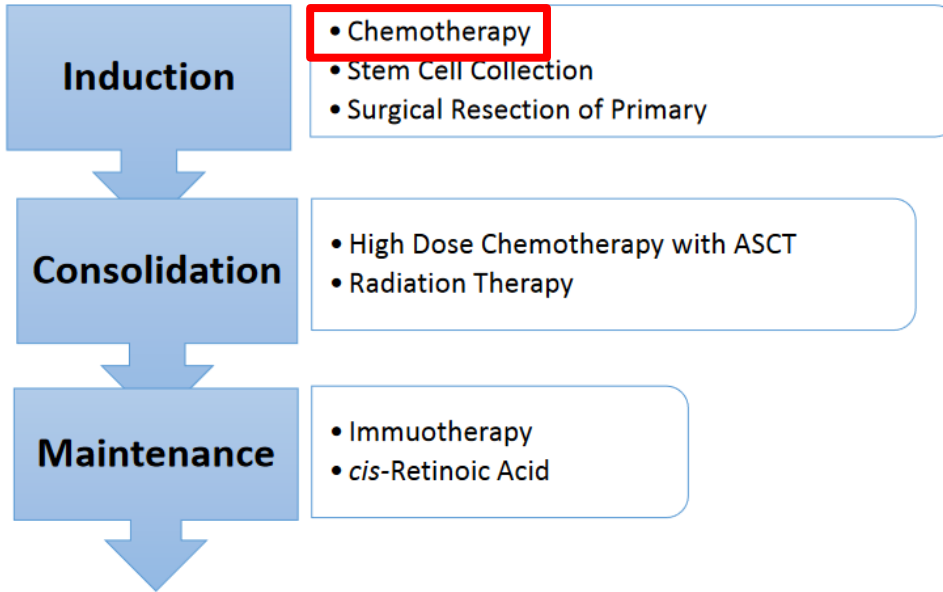


# Population-based approach

$$\text{Rate of change of a population size} = \text{Growth rate} - \text{Death rate} + \text{Immigration rate} - \text{Emigration rate}$$

# Induction chemotherapy

Current standard:  
multi-modal therapy.



COJEC protocol:

C: cisplatin.

O: vincristine.

J: carboplatin.

E: etoposide.

C: cyclophosphamide.

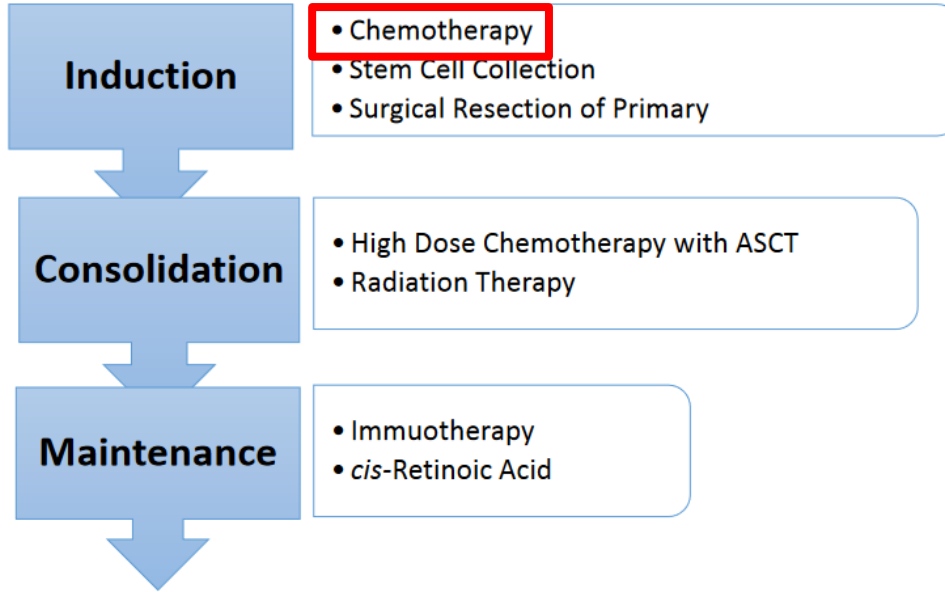
Eight two-week cycles.

- Alternating combinations.
- Maximum tolerated doses.

One protocol for every patient.

# Induction chemotherapy

Current standard:  
multi-modal therapy.



COJEC protocol:

C: cisplatin.

**O: vincristine.**

J: carboplatin.

E: etoposide.

**C: cyclophosphamide.**

Optimise a two-drug protocol.

- Number of cycles.
- Doses in each cycle.

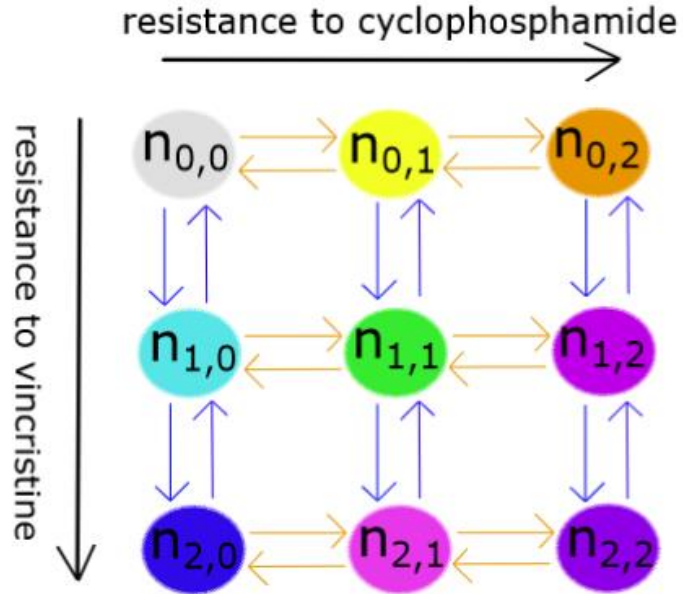
# Induction chemotherapy

Three levels of resistance  
against one drug.

Two drugs.

Therefore, nine  
populations.

# Model structure



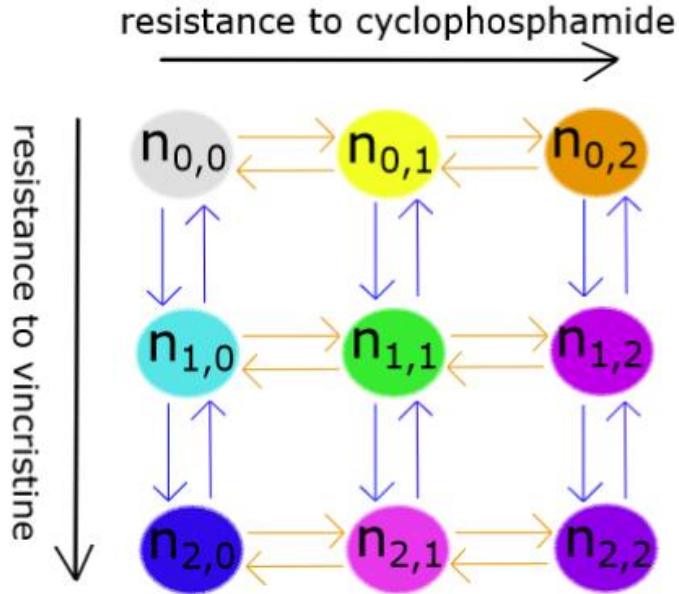
Italia, Matteo, et al. "Mathematical Model of Clonal Evolution Proposes a Personalised Multi-Modal Therapy for High-Risk Neuroblastoma." *Cancers* 15.7 (2023): 1986.

# Population-based approach

$$\text{Rate of change of a population size} = \text{Growth rate} - \text{Death rate} + \text{Immigration rate} - \text{Emigration rate}$$



# Model structure



Rate of change  
of a population  
size.

Growth  
rate.

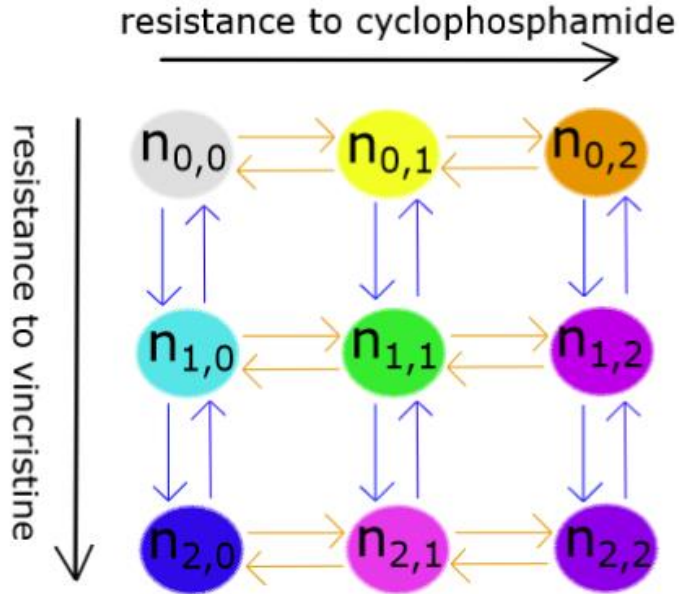
Net immigration  
or mutation rate.

Death  
rate.

$$\frac{dn_{i,j}(t)}{dt} = \frac{G(t)}{1 + \alpha_r \phi(\tau)} - \frac{M(t)}{1 + \alpha_r \phi(\tau)} - \frac{D(t)}{1 + \alpha_m \phi(\tau)}$$

One ordinary differential equation for each  
population (clone).

# Model structure



Rate of change of a population size.

Growth rate.

Net immigration or mutation rate.

Death rate.

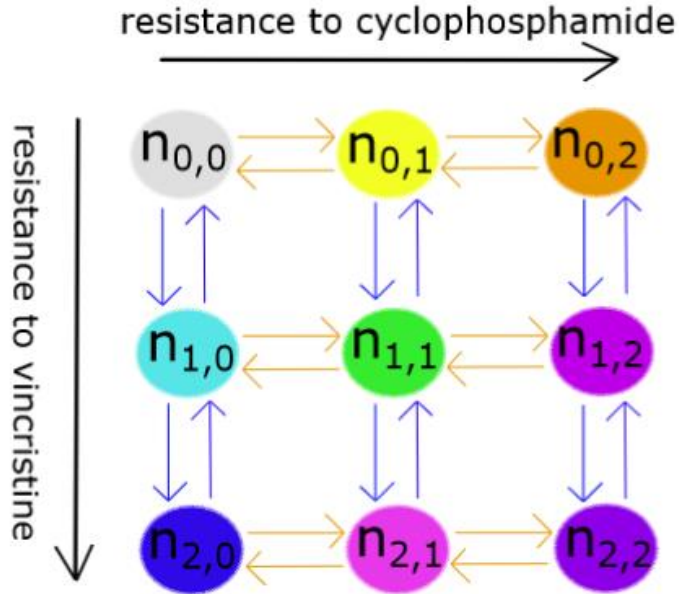
$$\frac{dn_{i,j}(t)}{dt} = \frac{G(t)}{1 + \alpha_r \phi(\tau)} - \frac{M(t)}{1 + \alpha_r \phi(\tau)} - \frac{D(t)}{1 + \alpha_m \phi(\tau)}$$

One ordinary differential equation for each population (clone).

$$G(t) = \left(1 - \frac{\sum_{k,l} n_{k,l}(t)}{K}\right) \left(r_{i,j} n_{i,j}(t)\right) \text{ is the logistic growth rate}$$

Ensures that the total population size cannot exceed an upper limit (carrying capacity).

# Model structure



Rate of change of a population size.

Growth rate.

Net immigration or mutation rate.

Death rate.

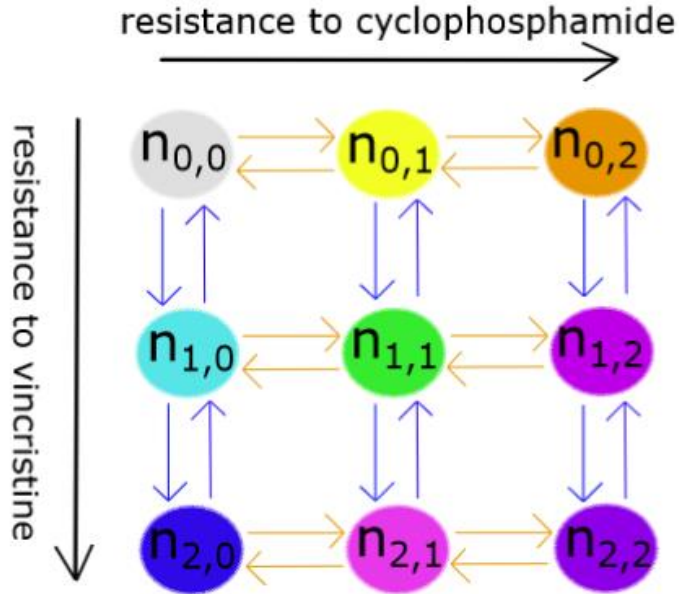
$$\frac{dn_{i,j}(t)}{dt} = \frac{G(t)}{1 + \alpha_r \phi(\tau)} - \frac{M(t)}{1 + \alpha_r \phi(\tau)} - \frac{D(t)}{1 + \alpha_m \phi(\tau)}$$

One ordinary differential equation for each population (clone).

$$G(t) = \left(1 - \frac{\sum_{k,l} n_{k,l}(t)}{K}\right) \left(r_{i,j} n_{i,j}(t)\right) \text{ is the logistic growth rate}$$

$$M(t) = \mu \left(1 - \frac{\sum_{k,l} n_{k,l}(t)}{K}\right) \left(\gamma_{i,j} r_{i,j} n_{i,j}(t) - \sum_{p,q} r_{p,q} n_{p,q}(t)\right)$$

# Model structure



Rate of change of a population size.

Growth rate.

Net immigration or mutation rate.

Death rate.

$$\frac{dn_{i,j}(t)}{dt} = \frac{G(t)}{1 + \alpha_r \phi(\tau)} - \frac{M(t)}{1 + \alpha_r \phi(\tau)} - \frac{D(t)}{1 + \alpha_m \phi(\tau)}$$

One ordinary differential equation for each population (clone).

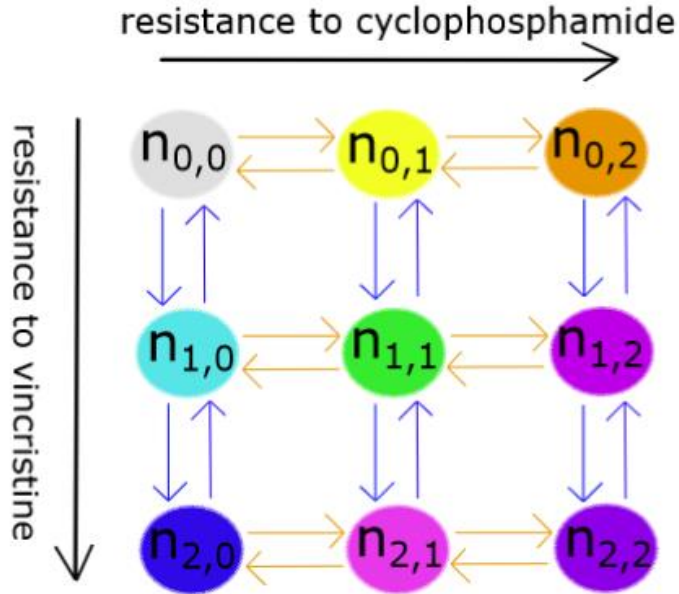
$$G(t) = \left(1 - \frac{\sum_{k,l} n_{k,l}(t)}{K}\right) \left(r_{i,j} n_{i,j}(t)\right) \text{ is the logistic growth rate}$$

$$M(t) = \mu \left(1 - \frac{\sum_{k,l} n_{k,l}(t)}{K}\right) \left(\gamma_{i,j} r_{i,j} n_{i,j}(t) - \sum_{p,q} r_{p,q} n_{p,q}(t)\right)$$

$$D(t) = \sum_d m_d^{i,j}(c_d(t)) n_{i,j}(t) \text{ is the rate of drug-induced death}$$

Therapy influences this term.

# Model structure



Italia, Matteo, et al. "Mathematical Model of Clonal Evolution Proposes a Personalised Multi-Modal Therapy for High-Risk Neuroblastoma." *Cancers* 15.7 (2023): 1986.

Rate of change of a population size.

Growth rate.

Net immigration or mutation rate.

Death rate.

$$\frac{dn_{i,j}(t)}{dt} = \frac{G(t)}{1 + \alpha_r \phi(\tau)} - \frac{M(t)}{1 + \alpha_r \phi(\tau)} - \frac{D(t)}{1 + \alpha_m \phi(\tau)}$$

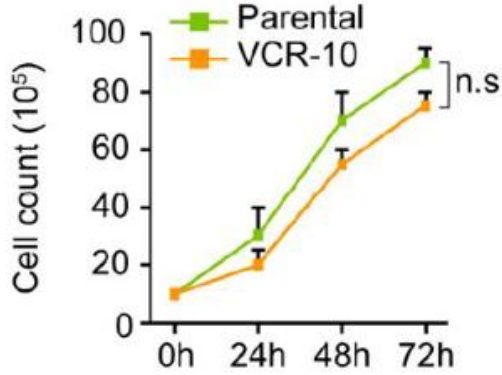
One ordinary differential equation for each population (clone).

$$\frac{dc_d(t)}{dt} = \omega_d(t) - z_d c_d(t), \quad d = 1, 2$$

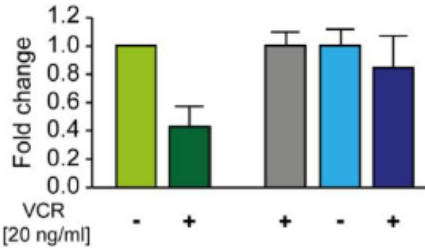
One first-order pharmacokinetic equation for each drug. Vincristine and cyclophosphamide.

Setting a chemotherapy schedule means replacing this variable with a time series.

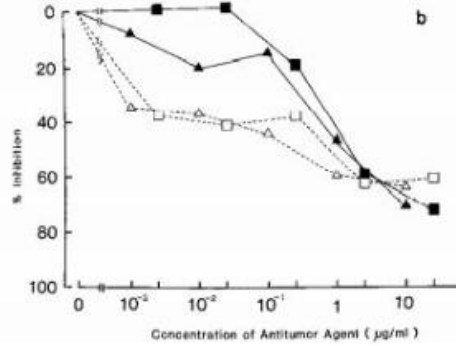
# Model calibration



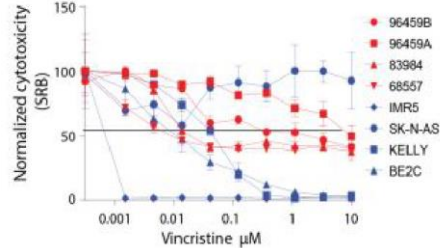
Jemaà, Mohamed, et al. "Gene expression signature of acquired chemoresistance in neuroblastoma cells." *International Journal of Molecular Sciences* 21.18 (2020): 6811.



Jemaà, Mohamed, et al. "Gene expression signature of acquired chemoresistance in neuroblastoma cells." *International Journal of Molecular Sciences* 21.18 (2020): 6811.

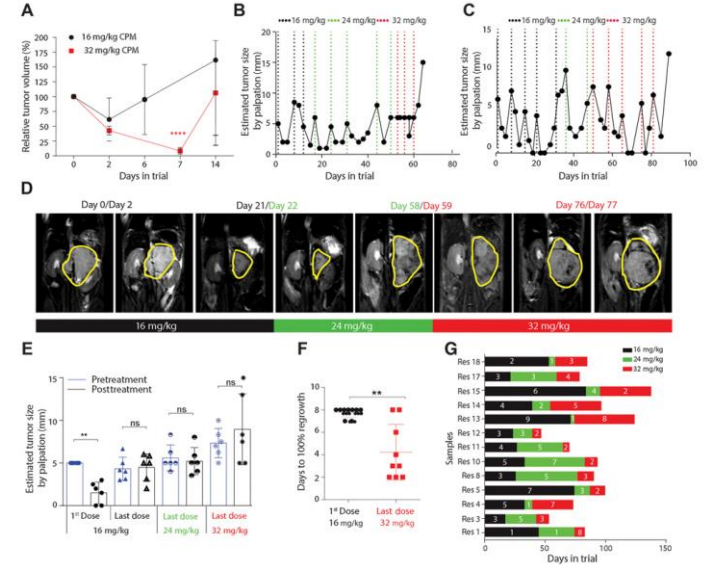


Zaizen, Y., A. Nakagawara, and K. Ikeda. "Patterns of destruction of mouse neuroblastoma cells by extracellular hydrogen peroxide formed by 6-hydroxydopamine and ascorbate." *Journal of cancer research and clinical oncology* 111 (1986): 93-97.



Yogev, Orli, et al. "In Vivo Modeling of Chemoresistant Neuroblastoma Provides New Insights into Chemorefractory Disease and Metastasis." *Cancer research* 79.20 (2019): 5382-5393.

Levenberg-Marquardt algorithm.  
Local optimisation method.



Yogev, Orli, et al. "In Vivo Modeling of Chemoresistant Neuroblastoma Provides New Insights into Chemorefractory Disease and Metastasis." *Cancer research* 79.20 (2019): 5382-5393.

# Optimisation

One schedule, 24 doses.

One chromosome, 24 genes.

0.1	0.5	1.9	0.2	0.6	0.7	1.1	0.2	1.5	0.4	0.3	1.7	1.1	0.1	0.9	0.6	1.3	0.2	0.3	1.6	0.1	0.7	1.8	0.3
-----	-----	-----	-----	-----	-----	-----	-----	-----	-----	-----	-----	-----	-----	-----	-----	-----	-----	-----	-----	-----	-----	-----	-----

Vincristine.

Cyclophosphamide.

# Optimisation

One schedule, 24 doses.

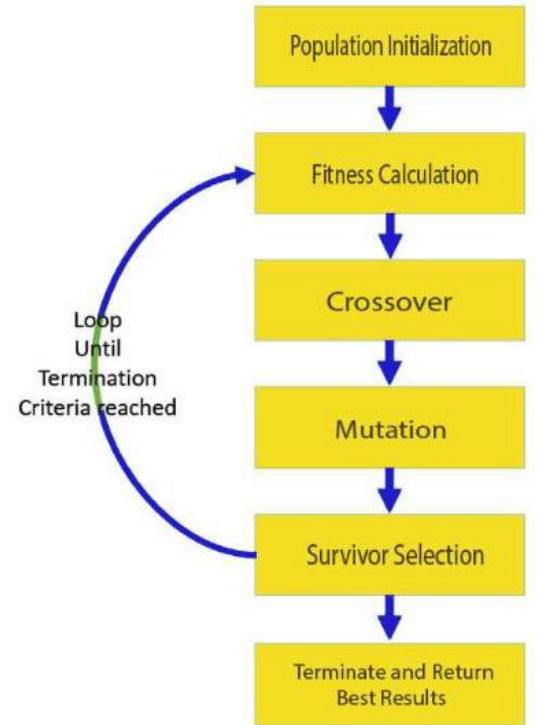
One chromosome, 24 genes.

0.1 0.5 1.9 0.2 0.6 0.7 1.1 0.2 1.5 0.4 0.3 1.7 1.1 0.1 0.9 0.6 1.3 0.2 0.3 1.6 0.1 0.7 1.8 0.3

Vincristine.

Cyclophosphamide.

Genetic algorithm.  
Global optimisation.





# Optimisation

One schedule, 24 doses.

One chromosome, 24 genes.

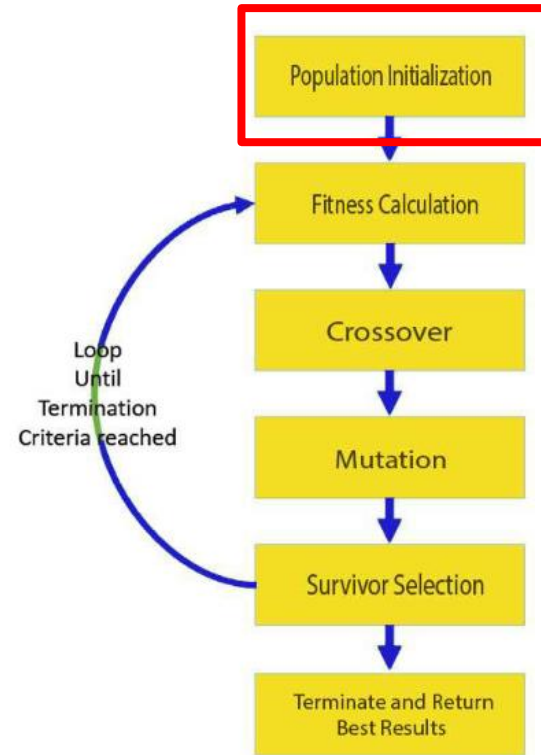


Vincristine.

Cyclophosphamide.

Create many (for example, 100) schedules or chromosomes.

Genetic algorithm.  
Global optimisation.



Haldurai, Lingaraj, T. Madhubala, and R. Rajalakshmi. "A study on genetic algorithm and its applications." *Int. J. Comput. Sci. Eng* 4.10 (2016): 139-143.

# Optimisation

One schedule, 24 doses.

One chromosome, 24 genes.

0.1 0.5 1.9 0.2 0.6 0.7 1.1 0.2 1.5 0.4 0.3 1.7 1.1 0.1 0.9 0.6 1.3 0.2 0.3 1.6 0.1 0.7 1.8 0.3

Vincristine.

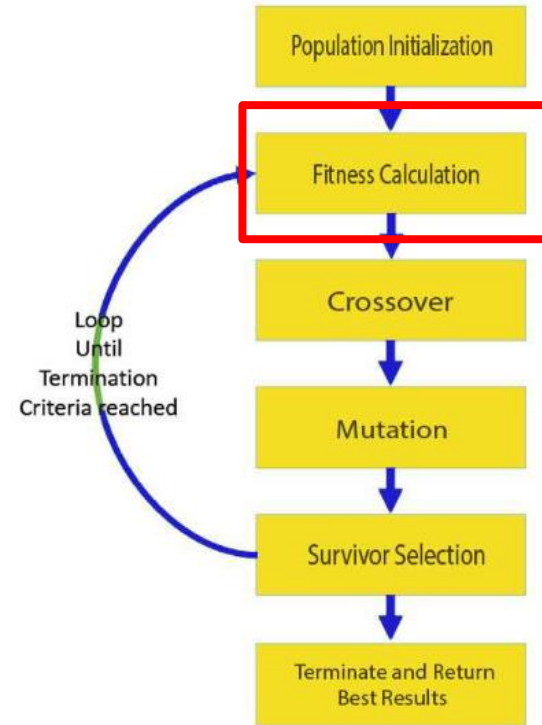
Cyclophosphamide.

$$\frac{dn_{i,j}(t)}{dt} = \frac{G(t)}{1 + \alpha_r \phi(\tau)} - \frac{M(t)}{1 + \alpha_r \phi(\tau)} - \frac{D(t)}{1 + \alpha_m \phi(\tau)}$$

$$\frac{dc_d(t)}{dt} = \omega_d(t) - z_d c_d(t), \quad d = 1, 2$$

Simulate the tumour's response to every chemotherapy.

Genetic algorithm.  
Global optimisation.



Haldurai, Lingaraj, T. Madhubala, and R. Rajalakshmi. "A study on genetic algorithm and its applications." *Int. J. Comput. Sci. Eng* 4.10 (2016): 139-143.

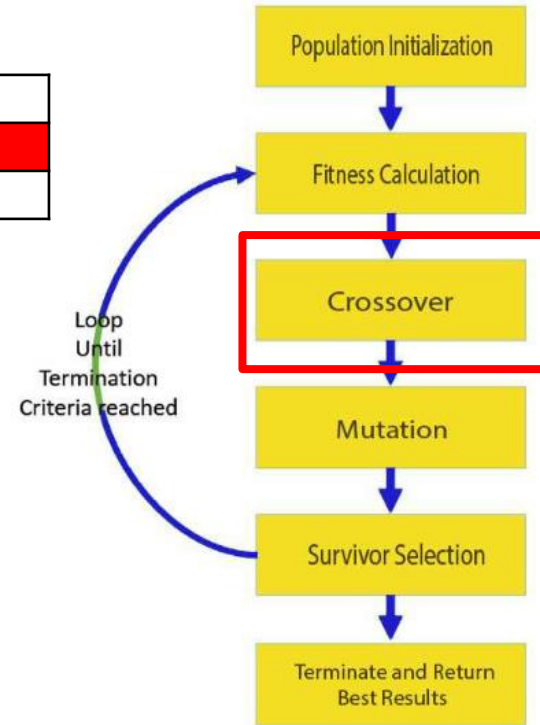
# Optimisation

Chromosome 1	1	2	3	4
Chromosome 2	5	6	7	8
Chromosome 3	1	2	7	8



Let the best chemotherapy schedules (chromosomes) combine.

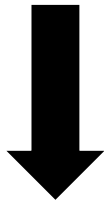
Genetic algorithm.  
Global optimisation.



Haldurai, Lingaraj, T. Madhubala, and R. Rajalakshmi. "A study on genetic algorithm and its applications." *Int. J. Comput. Sci. Eng* 4.10 (2016): 139-143.

# Optimisation

Chromosome 1	1	2	3	4
Chromosome 2	5	6	7	8
Chromosome 3	1	2	7	8

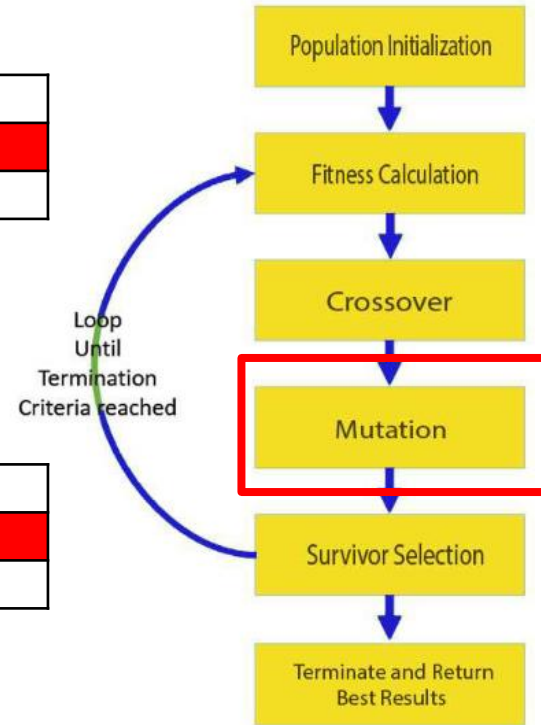


Random mutation.

Chromosome 1	1	2	3	4
Chromosome 2	5	6	7	8
Chromosome 3	9	2	7	8

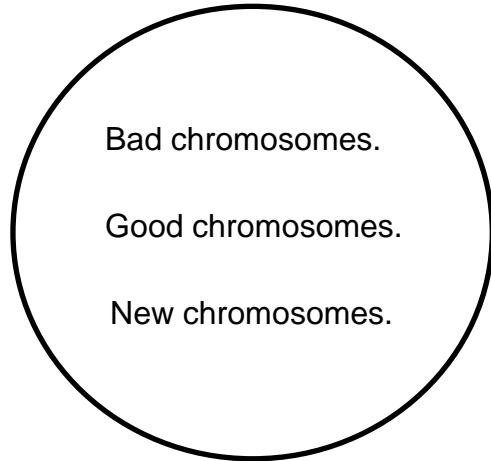
Random mutation diversifies the collection of schedules.

Genetic algorithm.  
Global optimisation.



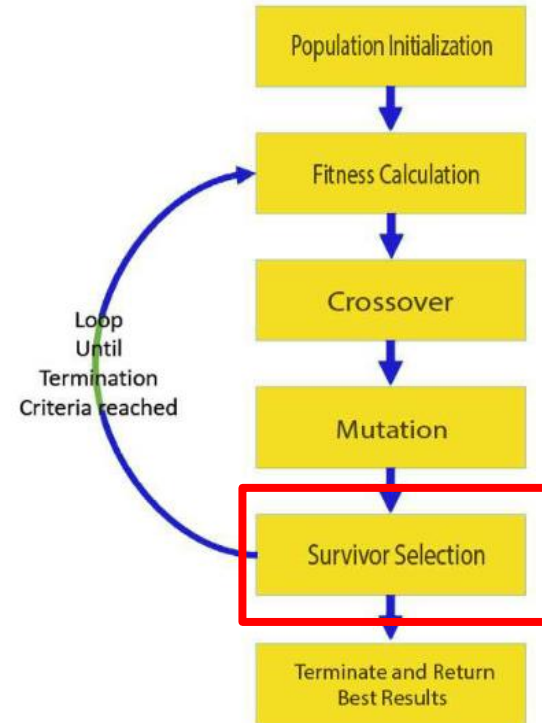
Haldurai, Lingaraj, T. Madhubala, and R. Rajalakshmi. "A study on genetic algorithm and its applications." *Int. J. Comput. Sci. Eng* 4.10 (2016): 139-143.

# Optimisation



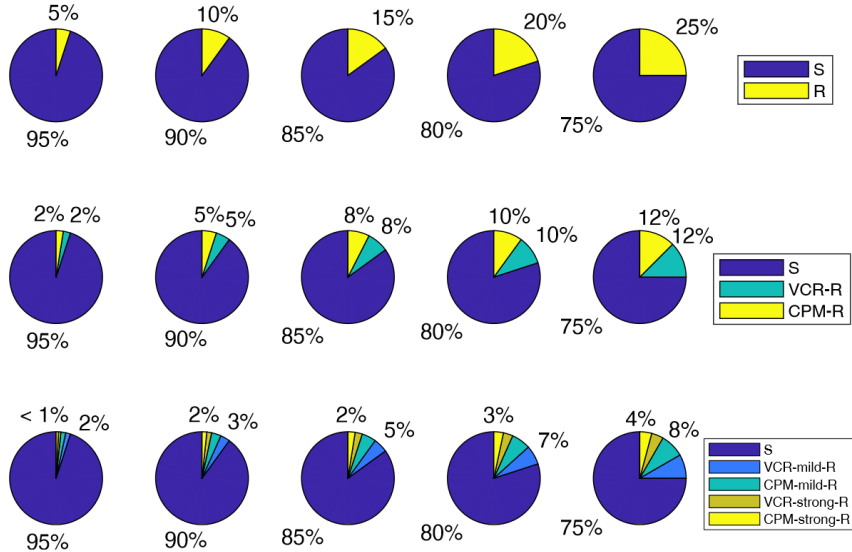
Sample from this collection to produce the next generation.

Genetic algorithm.  
Global optimisation.



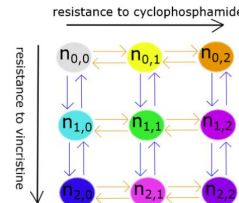
Haldurai, Lingaraj, T. Madhubala, and R. Rajalakshmi. "A study on genetic algorithm and its applications." *Int. J. Comput. Sci. Eng* 4.10 (2016): 139-143.

# Optimisation

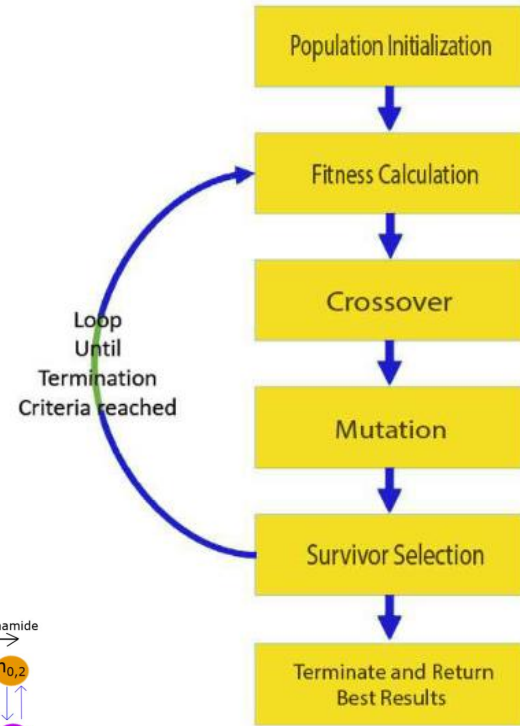


36 tumours with different compositions.

Different distributions of cells between the nine populations.



Genetic algorithm.  
Global optimisation.

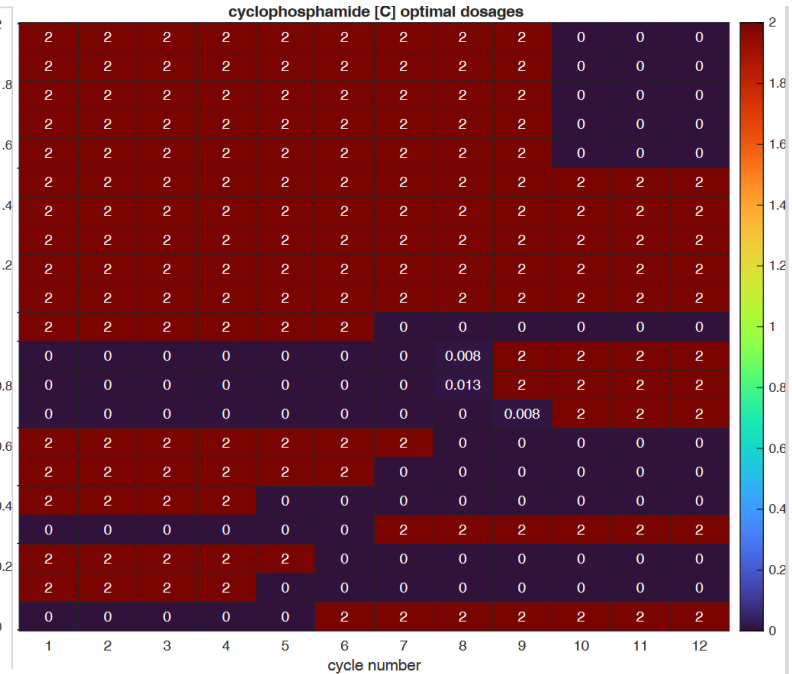
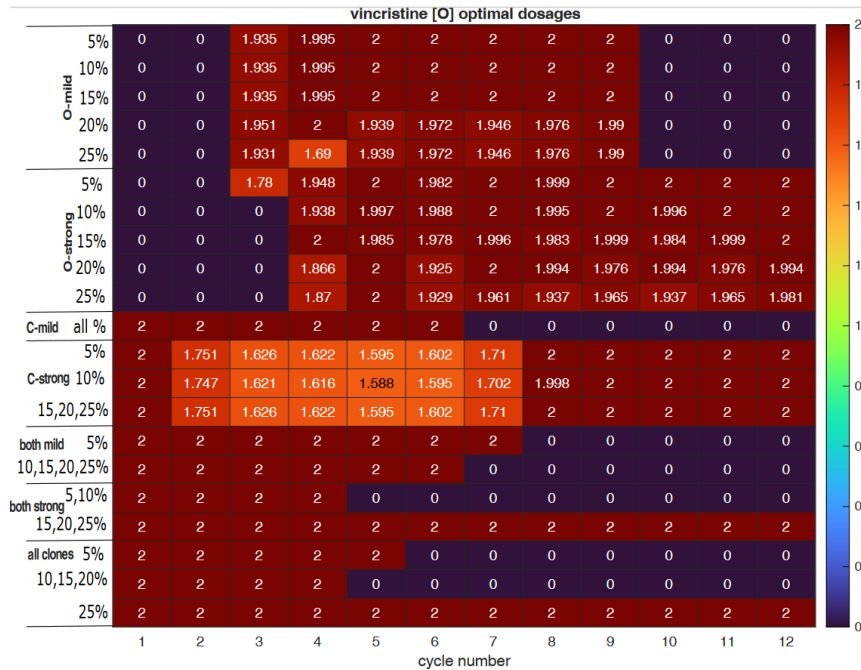


Haldurai, Lingaraj, T. Madhubala, and R. Rajalakshmi. "A study on genetic algorithm and its applications." *Int. J. Comput. Sci. Eng* 4.10 (2016): 139-143.



# Optimised schedules

When one drug is more effective than the other, evolutionary therapy only works for tumours with certain clonal compositions.





# Connections to Hull University Business School

Chemical Engineering Journal 158 (2010) 241–249



ELSEVIER

Contents lists available at ScienceDirect

Chemical Engineering Journal

journal homepage: [www.elsevier.com/locate/cej](http://www.elsevier.com/locate/cej)

Chemical  
Engineering  
Journal

## Dynamic modeling and process optimization of an industrial sulfuric acid plant

Anton A. Kiss<sup>a,\*</sup>, Costin S. Bildea<sup>b</sup>, Johan Grievink<sup>c</sup>

<sup>a</sup> AkzoNobel Research, Development and Innovation, Process & Product Technology, Velperweg 76, 6824 BM, Arnhem, The Netherlands

<sup>b</sup> University "Politehnica" Bucharest, Centre for Technology Transfer in Process Industries, Polizu 1-7, RO-011061 Bucharest, Romania

<sup>c</sup> Delft University of Technology, Department of Chemical Engineering, Julianalaan 136, 2628 BL, Delft, The Netherlands

### ARTICLE INFO

#### Article history:

Received 15 October 2009

Received in revised form 8 January 2010

Accepted 11 January 2010

#### Keywords:

Sulfuric acid

Adiabatic reactors

Absorption

Optimization

SOx emissions

Energy savings

### ABSTRACT

The current legislation imposes tighter restrictions in order to reduce the impact of chemical process industry on the environment. In this context, this study presents the dynamic model, simulation and optimization results for an industrial sulfuric acid plant. The dynamic model, implemented in PSE gPROMS includes a catalytic reactor (five pass converter), heat exchangers such as economizers and feed-effluent heat exchangers, mixers, splitters and reactive absorption columns. The kinetic parameters were fitted to the real plant data, while the remaining model parameters were estimated using classical correlations. The modeling results agree very well with the real plant data.

The model implemented in gPROMS is useful for evaluating the dynamic behavior of the plant and for minimization of the total amount of SOx emissions. The SOx emissions could be significantly reduced by over 40% by optimizing operating parameters such as air feed flow rates or split fractions. However, only minor increases in energy production can be achieved due to the plant already operating near full capacity. The simulations also show that operational problems may occur when the process is disturbed due to production rate changes or catalyst deactivation, the non-linear response of the plant leading to sustained oscillations. Besides controllability, operability and optimization studies the gPROMS plant model is also useful for operator training and various scenario assessments.

© 2010 Elsevier B.V. All rights reserved.

Applied Mathematics and Computation 388 (2021) 125464

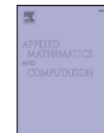


ELSEVIER

Contents lists available at ScienceDirect

Applied Mathematics and Computation

journal homepage: [www.elsevier.com/locate/amc](http://www.elsevier.com/locate/amc)



## Short communication

## Numerical schemes and genetic algorithms for the optimal control of a continuous model of supply chains

Luigi Rarità<sup>a,\*</sup>, Ivanka Stamova<sup>b</sup>, Stefania Tomasiello<sup>c</sup>

<sup>a</sup> Dipartimento di Ingegneria Industriale, Università degli Studi di Salerno, via Giovanni Paolo II, 132, Fisciano 84084, Italy

<sup>b</sup> Department of Mathematics, University of Texas at San Antonio, San Antonio, TX 78249, USA

<sup>c</sup> Institute of Computer Science, University of Tartu, Narva mnt 18, Tartu 51008, Estonia



### ARTICLE INFO

#### Article history:

Received 3 January 2020

Revised 27 May 2020

Accepted 8 June 2020

Available online 22 July 2020

#### Keywords:

Upwind

Differential quadrature

Genetic algorithms

Supply chains

### ABSTRACT

In this paper, we consider supply chains modelled by partial and ordinary differential equations, for densities of parts on suppliers and queues among consecutive arcs, respectively. The considered numerical schemes, whose properties are discussed, foresee the upwind method for goods densities, described by conservation laws, and a Differential Quadrature based explicit formula for queues evolutions. An optimization scheme is also discussed, by considering a cost functional that, according to a pre-defined outflow, weights the queues through variations of processing velocities of suppliers. We get the minimization of the cost functional via a genetic algorithm, which uses mechanisms of selection, crossover and mutation for the processing velocities. An example application is discussed in light of the numerical approaches and the optimization procedure.

© 2020 Elsevier Inc. All rights reserved.

Kiss, Anton A., Costin S. Bildea, and Johan Grievink. "Dynamic modeling and process optimization of an industrial sulfuric acid plant." *Chemical Engineering Journal* 158.2 (2010): 241-249.

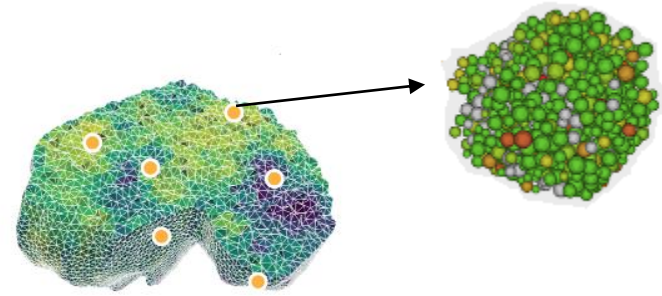
Rarità, Luigi, Ivanka Stamova, and Stefania Tomasiello. "Numerical schemes and genetic algorithms for the optimal control of a continuous model of supply chains." *Applied Mathematics and Computation* 388 (2021): 125464.

# Lecture outline

- ~~1. Neuroblastoma.~~
- ~~2. Multiscale problem.~~
- ~~3. Tumour scale.~~
- 4. Tissue scale.**
5. Cellular scale.

# Individual-based approach

Scale: Patch of a tumour (tissue level).



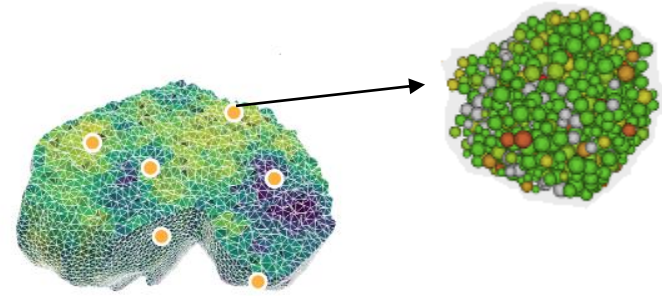
# Individual-based approach

Scale: Patch of a tumour (tissue level).

Resolution: Single cell.

A tumour region is represented by discrete cellular agents with spatial coordinates and other attributes, such as mutations.

They behave stochastically.



# Individual-based approach

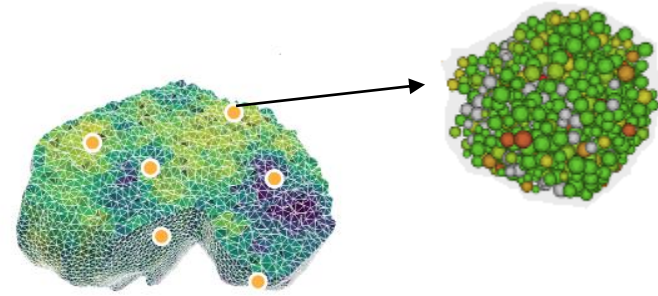
Scale: Patch of a tumour (tissue level).

Resolution: Single cell.

A tumour region is represented by discrete cellular agents with spatial coordinates and other attributes, such as mutations.

They behave stochastically.

Modelling framework: Agent-based models.



# Individual-based approach

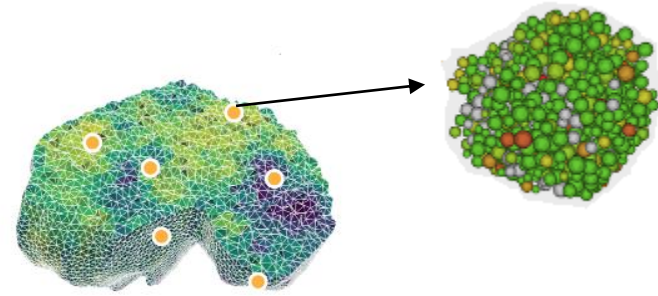
Scale: Patch of a tumour (tissue level).

Resolution: Single cell.

A tumour region is represented by discrete cellular agents with spatial coordinates and other attributes, such as mutations.

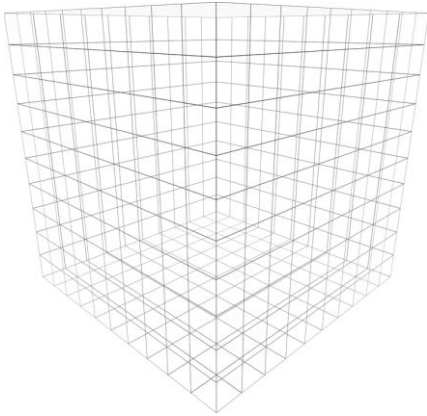
They behave stochastically.

Modelling framework: Agent-based models.



They are computationally expensive to implement.

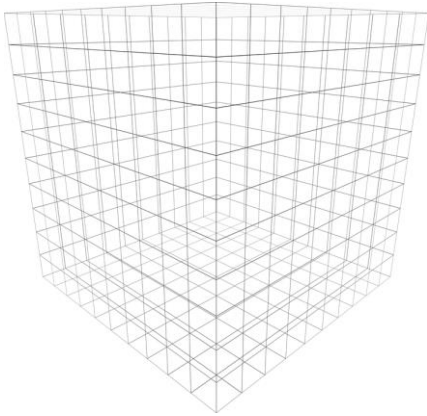
# Model structure



Continuous automaton to  
voxelate the microenvironment.

1. Spatial distributions of cells  
and extracellular matrix.
2. Concentration dynamics of  
drugs and nutrients (uniform).

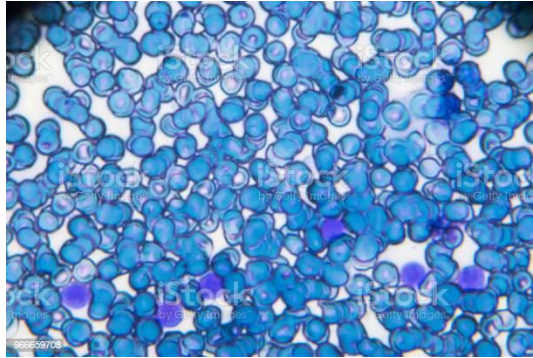
# Model structure



Continuous automaton to voxelate the microenvironment.

1. Spatial distributions of cells and extracellular matrix.

2. Concentration dynamics of drugs and nutrients (uniform).

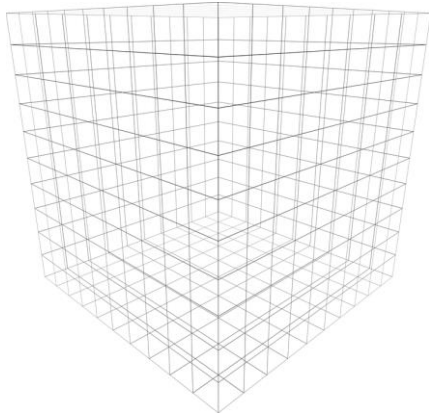


Discrete agents.

1. Neuroblastoma and Schwann cells.
2. Cell cycling and death.

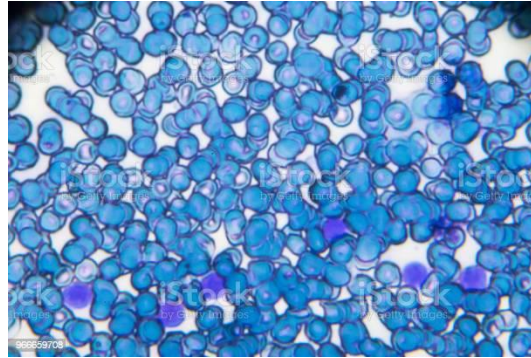


# Model structure



Continuous automaton to voxelate the microenvironment.

1. Spatial distributions of cells and extracellular matrix.
2. Concentration dynamics of drugs and nutrients (uniform).



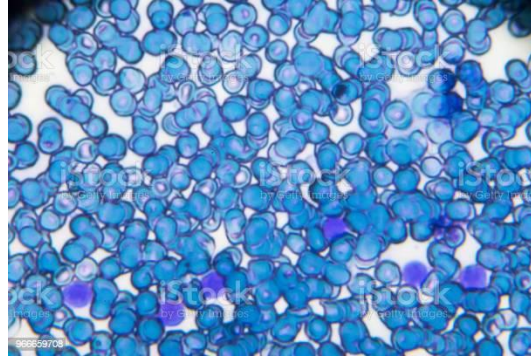
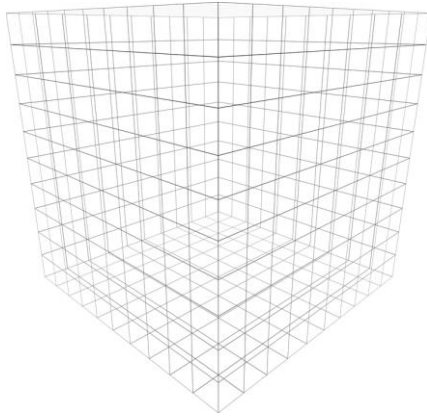
Discrete agents.

1. Neuroblastoma and Schwann cells.
2. Cell cycling and death.

Agent attributes.

1. Mutations.
2. DNA status.
3. Gene expression levels.

# Model structure



Continuous automaton to voxelate the microenvironment.

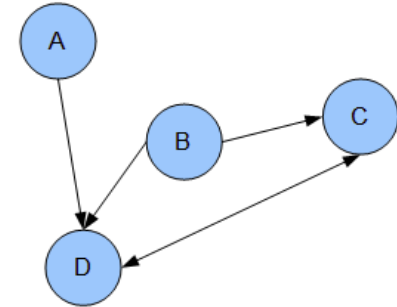
1. Spatial distributions of cells and extracellular matrix.
2. Concentration dynamics of drugs and nutrients (uniform).

Discrete agents.

1. Neuroblastoma and Schwann cells.
2. Cell cycling and death.

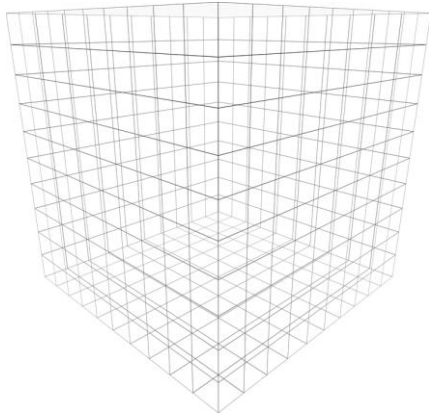
Agent attributes.

1. Mutations.
2. DNA status.
3. **Gene expression levels.**



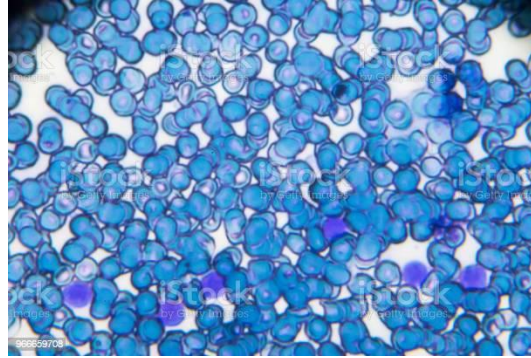
20 gene products. Telomerase, ALT, MYCN, MAPK/RAS pathway, JAB1, CHK1, CDS1, CDC25C, ID2, IAP2, HIF, BNIP3, VEGF, p53, p73, p21, p27, Bcl-2/Bcl-xL, BAK/BAX, and CAS.

# Model structure



Continuous automaton to voxelate the microenvironment.

1. Spatial distributions of cells and extracellular matrix.
2. Concentration dynamics of drugs and nutrients (uniform).

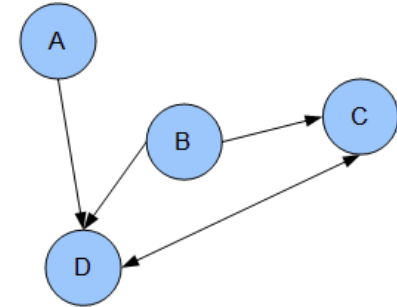
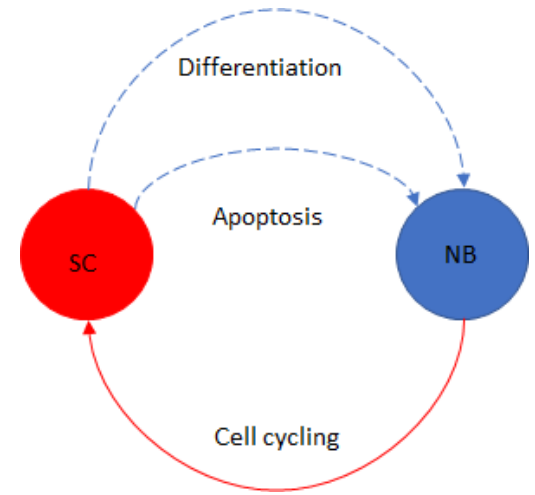


Discrete agents.

1. Neuroblastoma and Schwann cells.
2. Cell cycling and death.

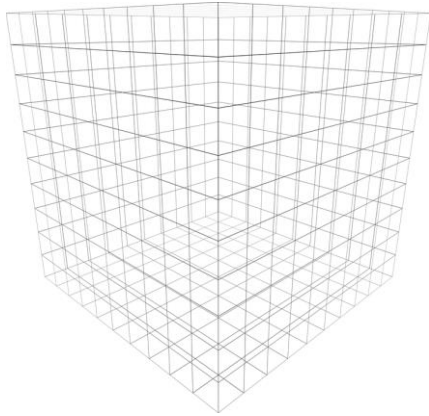
Agent attributes.

1. Mutations.
2. DNA status.
3. Gene expression levels.



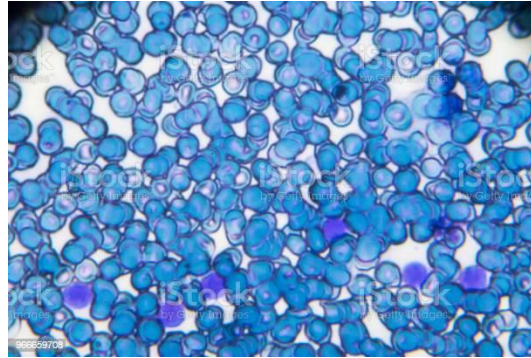
20 gene products. Telomerase, ALT, MYCN, MAPK/RAS pathway, JAB1, CHK1, CDS1, CDC25C, ID2, IAP2, HIF, BNIP3, VEGF, p53, p73, p21, p27, Bcl-2/Bcl-xL, BAK/BAX, and CAS.

# Model structure



Continuous automaton to voxelate the microenvironment.

1. Spatial distributions of cells and extracellular matrix.
2. Concentration dynamics of drugs and nutrients (uniform).

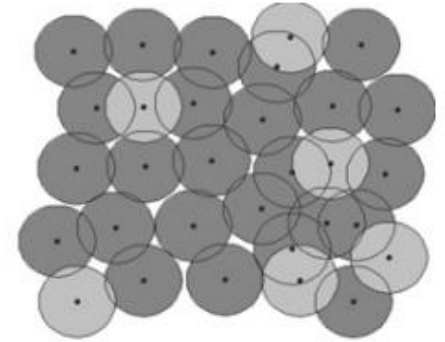


Discrete agents.

1. Neuroblastoma and Schwann cells.
2. Cell cycling and death.

Agent attributes.

1. Mutations.
2. DNA status.
3. Gene expression levels.



Centre-based mechanical model.

1. Resolve agent-agent overlap and contact inhibition.
2. Linear force law.
3. Equation of motion.

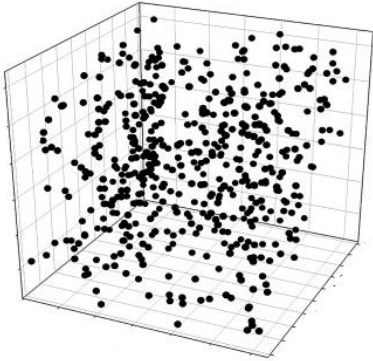
# Stochastic simulation algorithm

1. Each agent senses the microenvironment and its neighbouring agents, modifies its behaviour, and updates its attributes.
2. Resolve agent-agent overlap using the mechanical model.
3. Modify the microenvironment by considering the agents collectively.
4. Back to step 1.

A series of Bernoulli trials. For example, is the MAPK/RAS pathway active?



# Model calibration

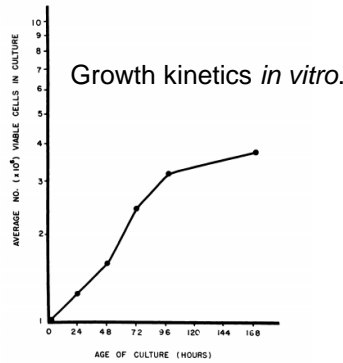


Latin hypercube sampling.

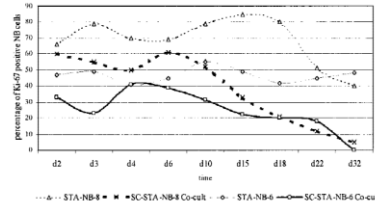
1. 3000 combinations of 20 fitting parameters (not entirely corresponding to the 20 gene products).

2. Minimised differences between simulation results and *in vitro* data.

3. Refinement for *in vivo* use.



Tumilowicz, Joseph J., et al. "Definition of a continuous human cell line derived from neuroblastoma." *Cancer research* 30.8 (1970): 2110-2118.



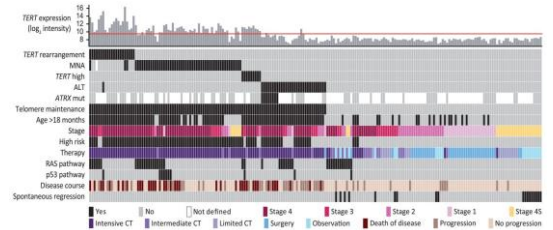
Ambros, Ingeborg M., et al. "Neuroblastoma cells provoke Schwann cell proliferation *in vitro*." *Medical and Pediatric Oncology: The Official Journal of SIOP—International Society of Pediatric Oncology (Société Internationale d'Oncologie Pédiatrique)* 36.1 (2001): 163-168.

Interactions between neuroblastoma and Schwann cells *in vitro*.

	Three-stage fit	95% CI	Direct fit	95% CI
Maximum oxygen consumption rate, $q_{max}$ (mmHg · s <sup>-1</sup> )	17.5	15.3–25.1	16.3	15.3–17.9
$P_{O_2}$ for 50% drop in consumption, $P_{50,q}$ (mmHg)	2.7	0.0–12.5	1.6	1.2–2.1
Maximum misonidazole binding rate, $k_{b,0}$ ( $\times 10^{-4}$ s <sup>-1</sup> )	4.5	3.9–4.9	4.4	2.5–5.3
$P_{O_2}$ for 50% drop in binding, $P_{50,b}$ (mmHg)	1.4	0.3–2.6	1.4	1.1–2.5
$P_{O_2}$ for 50% necrosis, $P_{50,n}$ (mmHg)	1.2	0.1–4.9	1.0	0.4–1.2

Warren, Daniel R., and Mike Partridge. "The role of necrosis, acute hypoxia and chronic hypoxia in 18F-FMISO PET image contrast: a computational modelling study." *Physics in Medicine & Biology* 61.24 (2016): 8596.

Extent of necrosis during hypoxia *in vitro*.

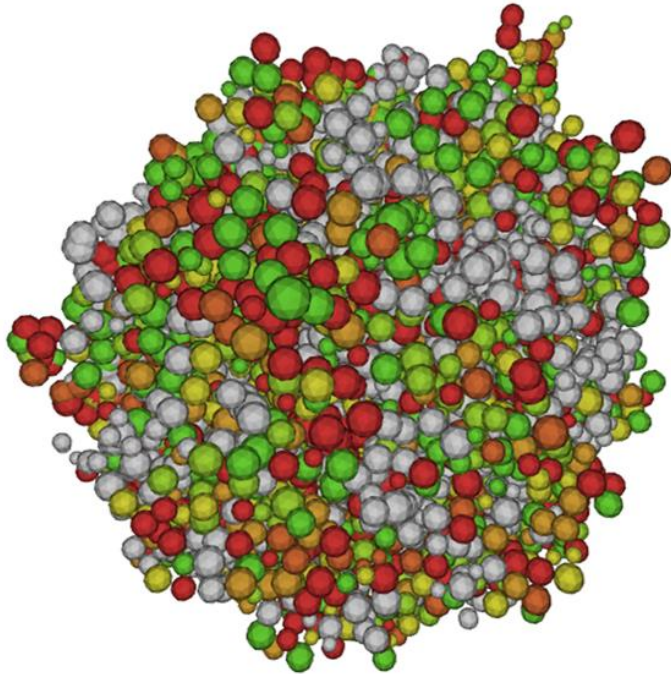


Ackermann, Sandra, et al. "A mechanistic classification of clinical phenotypes in neuroblastoma." *Science* 362.6419 (2018): 1165-1170.

Clinical outcomes associated with different mutations.



# Model calibration



Costly simulations.

1. Millions of agents.
2. Four months in a patient's life.
3. Stochastic simulations.

Simulations on GPUs.

1. FLAMEGPU and FLAMEGPU2 were used to generate optimised CUDA code.
2. 3000 time steps took up to 10 minutes.
3. Calibration took 40 days in total.

Hardware: 2 TITAN V GPUs, 1 TITAN XP GPU, and 1 TITAN RTX GPU.





# Connections to Hull University Business School

---

## An agent-based model for diffusion of electric vehicles

Ayla Kangur<sup>a</sup>, Wander Jager<sup>c</sup>  , Rineke Verbrugge<sup>a</sup> , Marija Bockarjova<sup>b</sup>

Show more 

+ Add to Mendeley  Share  Cite

---

<https://doi.org/10.1016/j.jenvp.2017.01.002>

[Get rights and content](#) 

### Abstract

The transition from fuel cars to electric cars is a large-scale process involving many interactions between consumers and other stakeholders over decades. To explore how policies may interact with consumer behavior over such a long time period, we developed an agent-based social simulation model. In this model, detailed data of 1795 respondents have been used to parameterise an agent architecture that addresses different consumer needs and decision strategies. Numerical experiments indicate that effective policy requires a long-lasting implementation of a combination of monetary, structural and informational measures. The strongest effect on emission reduction requires an exclusive support for full battery electric cars and no support for hybrid cars.

Kangur, Ayla, et al. "An agent-based model for diffusion of electric vehicles." *Journal of Environmental Psychology* 52 (2017): 166-182.



Virtual drug trials

Set parameters and initial conditions  
to model a highly malignant tumour.

Virtual drug trials

Simulated the effects of 5000 drug combinations on it.

## Virtual drug trials

Each drug combination has its own inhibitory effects on 20 gene products.

# Outcomes of virtual drug trials

Drug combination	MYCN_tt	APK_RAS	JAB1_tt	CHK1_tt	ID2_tt	IAP2_tt	HIF_tt	BNIP3_tt	VEGF_tt	p53_tt	p73_tt	p21_tt	p27_tt	cl2_Bclxl	AK_BAX_t	CAS_tt	CDS1_tt	CDC25C_tt	ALT_tt	telo_tt	Final cell count
1	0.672588	0.512894	0.549193	0.966997	0.730361	0.307462	0.207905	0.292707	0.274859	0.847529	0.95488	0.208644	0.829709	0.314768	0.306795	0.548809	0.512795	0.806082	0.239139	0.057796	2.9
2	0.370603	0.948461	0.176693	0.182967	0.9589	0.166757	0.662312	0.707124	0.517833	0.278251	0.330656	0.703401	0.926063	0.486678	0.728975	0.824148	0.330991	0.479153	0.625507	0.914947	810979.3
3	0.480702	0.361613	0.701094	0.691937	0.813686	0.56916	0.491749	0.194628	0.763884	0.635009	0.425961	0.600227	0.355538	0.096703	0.136706	0.207651	0.277639	0.599995	0.50865	0.299654	142367.9
4	0.114084	0.144439	0.055132	0.720272	0.062027	0.258779	0.353084	0.038602	0.636473	0.85034	0.803429	0.924868	0.806181	0.358857	0.007142	0.50443	0.297825	0.694638	0.448853	0.702866	1930.3
5	0.034541	0.755474	0.851892	0.219441	0.532749	0.382035	0.066466	0.493516	0.647967	0.1401	0.069769	0.103546	0.557345	0.345038	0.621808	0.417813	0.25704	0.858238	0.463051	0.119752	1022543.1
6	0.095174	0.264544	0.763187	0.237975	0.777168	0.759107	0.679167	0.930711	0.025504	0.561014	0.741876	0.167188	0.229481	0.677271	0.090438	0.228749	0.159534	0.498667	0.330174	0.327726	142986.9
7	0.072211	0.405286	0.679865	0.244582	0.655404	0.881224	0.765482	0.387844	0.259324	0.230217	0.631757	0.798782	0.48252	0.690296	0.576038	0.269205	0.564905	0.778981	0.002709	0.362195	435687
8	0.614301	0.030133	0.438368	0.278514	0.940645	0.057301	0.137183	0.288619	0.077186	0.171776	0.079315	0.670364	0.770426	0.3616	0.738607	0.089141	0.1277	0.287163	0.570988	0.260977	1064446.7
9	0.949785	0.726212	0.2906	0.655646	0.320445	0.038351	0.48271	0.425214	0.835405	0.533786	0.526146	0.35036	0.901427	0.128904	0.929766	0.559786	0.550643	0.628759	0.751473	0.029881	184403.7
10	0.536945	0.386602	0.825485	0.759076	0.523664	0.500507	0.333662	0.463655	0.713221	0.710428	0.92543	0.440239	0.301236	0.169734	0.230917	0.823692	0.38991	0.41621	0.138353	0.036424	2130.4
11	0.22587	0.599686	0.789976	0.598144	0.503783	0.202526	0.873167	0.586042	0.934024	0.138624	0.951306	0.980708	0.808283	0.530401	0.896325	0.840313	0.51384	0.832067	0.854344	0.454165	79487.9
12	0.64695	0.897711	0.965634	0.201915	0.297993	0.186404	0.84866	0.559633	0.651441	0.793313	0.8135	0.646678	0.414401	0.408218	0.029729	0.471666	0.855177	0.727191	0.049282	0.272398	16034.6
13	0.005338	0.682572	0.053721	0.776701	0.903579	0.312147	0.77007	0.605628	0.326107	0.619283	0.552992	0.76291	0.51865	0.250861	0.793856	0.316342	0.990211	0.501077	0.309332	0.704286	40082.2
14	0.154811	0.606159	0.99643	0.443671	0.121497	0.135064	0.498195	0.336761	0.585824	0.358976	0.11924	0.082192	0.169138	0.67295	0.040341	0.358252	0.309095	0.395602	0.45065	0.157112	785229.7
15	0.006523	0.371605	0.024329	0.275044	0.981941	0.844997	0.785737	0.4105	0.261254	0.421361	0.514435	0.273033	0.152655	0.894049	0.893089	0.133716	0.352879	0.931411	0.979398	0.725151	559332.2
16	0.035398	0.59838	0.921767	0.798465	0.529747	0.872198	0.110947	0.868952	0.212872	0.085575	0.280361	0.529599	0.534797	0.939852	0.422657	0.908396	0.676884	0.655001	0.590875	0.823192	448831
17	0.181127	0.66959	0.14328	0.929367	0.643068	0.132443	0.954782	0.8321	0.50553	0.687374	0.020436	0.33655	0.28789	0.476686	0.916698	0.864843	0.272412	0.721855	0.312538	0.249966	13375.3
18	0.16759	0.387294	0.450688	0.466438	0.451219	0.781471	0.832622	0.520067	0.412082	0.973701	0.779906	0.00505	0.537775	0.608167	0.295482	0.136452	0.269988	0.639514	0.638172	0.154891	8152.4
19	0.297731	0.951013	0.505903	0.781766	0.116431	0.984011	0.785794	0.560181	0.524662	0.841497	0.130318	0.026851	0.027742	0.179907	0.195185	0.275405	0.340416	0.633955	0.217325	0.041692	250378.3
20	0.910742	0.389507	0.913851	0.731569	0.530669	0.013639	0.526046	0.23999	0.182731	0.536673	0.532311	0.283933	0.135212	0.370857	0.285595	0.802866	0.189796	0.382408	0.256439	0.58473	178938.2
21	0.615935	0.913412	0.208502	0.242087	0.254474	0.659763	0.478573	0.386769	0.740985	0.802727	0.51063	0.872295	0.157521	0.64195	0.098882	0.334707	0.854887	0.444788	0.001647	0.699772	290863.5
22	0.88471	0.577089	0.739674	0.778813	0.495382	0.339487	0.849549	0.685108	0.755225	0.755025	0.077707	0.729292	0.302625	0.220438	0.262007	0.326127	0.559438	0.956624	0.131881	0.474293	81208.4
23	0.991051	0.87196	0.705799	0.942731	0.972844	0.926689	0.961589	0.307812	0.519009	0.763141	0.15985	0.217541	0.483494	0.820264	0.505629	0.829053	0.571262	0.677363	0.128252	0.53163	1312.8

Tabular dataset:

- 5000 rows/examples.
- 5000 drug combinations.

# Outcomes of virtual drug trials

Drug combination	MYCN_tt	APK_RAS	JAB1_tt	CHK1_tt	ID2_tt	IAP2_tt	HIF_tt	BNIP3_tt	VEGF_tt	p53_tt	p73_tt	p21_tt	p27_tt	cl2_Bclxl	AK_BAX_t	CAS_tt	CDS1_tt	CDC25C_tt	ALT_tt	telo_tt	Final cell count
1	0.672588	0.512894	0.549193	0.966997	0.730361	0.307462	0.207905	0.292707	0.274859	0.847529	0.95488	0.208644	0.829709	0.314768	0.306795	0.548809	0.512795	0.806082	0.239139	0.057796	2.9
2	0.370603	0.948461	0.176693	0.182967	0.9589	0.166757	0.662312	0.707124	0.517833	0.278251	0.330656	0.703401	0.926063	0.486678	0.728975	0.824148	0.330991	0.479153	0.625507	0.914947	810979.3
3	0.480702	0.361613	0.701094	0.691937	0.813686	0.56916	0.491749	0.194628	0.763884	0.635009	0.425961	0.600227	0.355538	0.096703	0.136706	0.207651	0.277639	0.599995	0.50865	0.299654	142367.9
4	0.114084	0.144439	0.055132	0.720272	0.062027	0.258779	0.353084	0.038602	0.636473	0.85034	0.803429	0.924868	0.806181	0.358857	0.007142	0.50443	0.297825	0.694638	0.448853	0.702866	1930.3
5	0.034541	0.755474	0.851892	0.219441	0.532749	0.382035	0.066466	0.493516	0.647967	0.1401	0.069769	0.103546	0.557345	0.345038	0.621808	0.417813	0.25704	0.858238	0.463051	0.119752	1022543.1
6	0.095174	0.264544	0.763187	0.237975	0.777168	0.759107	0.679167	0.930711	0.025504	0.561014	0.741876	0.167188	0.229481	0.677271	0.090438	0.228749	0.159534	0.498667	0.330174	0.327726	142986.9
7	0.072211	0.405286	0.679865	0.244582	0.655404	0.881224	0.765482	0.387844	0.259324	0.230217	0.631757	0.798782	0.48252	0.690296	0.576038	0.269205	0.564905	0.778981	0.002709	0.362195	435687
8	0.614301	0.030133	0.43868	0.278514	0.940645	0.057301	0.137183	0.288619	0.077186	0.171776	0.079315	0.670364	0.770426	0.3616	0.738607	0.089141	0.1277	0.287163	0.570988	0.260977	1064446.7
9	0.949785	0.726212	0.2906	0.655646	0.320445	0.038351	0.48271	0.425214	0.835405	0.533786	0.526146	0.35036	0.901427	0.128904	0.929766	0.559786	0.550643	0.628759	0.751473	0.029881	184403.7
10	0.536945	0.386602	0.825485	0.759076	0.523664	0.500507	0.333662	0.463655	0.713221	0.710428	0.92543	0.440239	0.301236	0.169734	0.230917	0.823692	0.38991	0.41621	0.138353	0.036424	2130.4
11	0.22587	0.599686	0.789976	0.598144	0.503783	0.202526	0.873167	0.586042	0.974024	0.138624	0.951306	0.980708	0.808283	0.530401	0.896325	0.840313	0.51384	0.832067	0.854344	0.454165	79487.9
12	0.64695	0.897711	0.965634	0.201915	0.297993	0.186404	0.84866	0.559633	0.651441	0.793313	0.8135	0.646678	0.414401	0.408218	0.029729	0.471666	0.855177	0.727191	0.049282	0.272398	16034.6
13	0.005338	0.682572	0.053721	0.776701	0.903579	0.312147	0.77007	0.605628	0.326107	0.619283	0.552992	0.76291	0.51865	0.250861	0.793856	0.316342	0.990211	0.501077	0.309332	0.704286	40082.2
14	0.154811	0.606159	0.99643	0.443671	0.121497	0.135064	0.498195	0.336761	0.585824	0.358976	0.11924	0.082192	0.169138	0.67295	0.040341	0.358252	0.309095	0.395602	0.45065	0.157112	785229.7
15	0.006523	0.371605	0.024329	0.275044	0.981941	0.844997	0.785737	0.4105	0.261254	0.421361	0.514435	0.273033	0.152655	0.894049	0.893089	0.133716	0.352879	0.931411	0.979398	0.725151	559332.2
16	0.035398	0.59838	0.921767	0.798465	0.529747	0.872198	0.110947	0.868952	0.212872	0.085575	0.280361	0.529599	0.534797	0.939852	0.422657	0.908396	0.676884	0.655001	0.590875	0.823192	448831
17	0.181127	0.66959	0.14328	0.929367	0.643068	0.132443	0.954782	0.8321	0.50553	0.687374	0.020436	0.33655	0.28789	0.476686	0.916698	0.864843	0.272412	0.721855	0.312538	0.249966	13375.3
18	0.16759	0.387294	0.450688	0.466438	0.451219	0.781471	0.832622	0.520067	0.412082	0.973701	0.779906	0.00505	0.537775	0.608167	0.295482	0.136452	0.269988	0.639514	0.638172	0.154891	8152.4
19	0.297731	0.951013	0.505903	0.781766	0.116431	0.984011	0.073974	0.560181	0.524662	0.841497	0.130318	0.026851	0.027742	0.179907	0.195185	0.275405	0.340416	0.633955	0.217325	0.041692	250378.3
20	0.910742	0.389507	0.913851	0.731569	0.530669	0.013639	0.526046	0.23999	0.182731	0.536673	0.532311	0.283933	0.135212	0.370857	0.285595	0.802866	0.189796	0.382408	0.256439	0.58473	178938.2
21	0.615935	0.913412	0.208502	0.242087	0.254474	0.659763	0.478573	0.386769	0.740985	0.802727	0.51063	0.872295	0.157521	0.64195	0.098882	0.334707	0.854887	0.444788	0.001647	0.699772	290863.5
22	0.88471	0.577089	0.739674	0.778813	0.495382	0.339487	0.849549	0.685108	0.755225	0.755025	0.077707	0.729292	0.302625	0.220438	0.262007	0.326127	0.559438	0.956624	0.131881	0.474293	81208.4
23	0.991051	0.87196	0.705799	0.942731	0.972844	0.926689	0.961589	0.307812	0.519009	0.763141	0.15985	0.217541	0.483494	0.820264	0.505629	0.829053	0.571262	0.677363	0.128252	0.53163	1312.8

Tabular dataset:

- 20 features/predictors.
- Inhibitory effects on 20 drug targets.

# Outcomes of virtual drug trials

Drug combination	MYCN_tt	APK_RAS	JAB1_tt	CHK1_tt	ID2_tt	IAP2_tt	HIF_tt	BNIP3_tt	VEGF_tt	p53_tt	p73_tt	p21_tt	p27_tt	cl2_Bclxl	BAK_BAX_t	CAS_tt	CDS1_tt	CDC25C_tt	ALT_tt	telo_tt	Final cell count
1	0.672588	0.512894	0.549193	0.966997	0.730361	0.307462	0.207905	0.292707	0.274859	0.847529	0.95488	0.208644	0.829709	0.314768	0.306795	0.548809	0.512795	0.806082	0.239139	0.057796	2.9
2	0.370603	0.948461	0.176693	0.182967	0.9589	0.166757	0.662312	0.707124	0.517833	0.278251	0.330656	0.703401	0.926063	0.486678	0.728975	0.824148	0.330991	0.479153	0.625507	0.914947	810979.3
3	0.480702	0.361613	0.701094	0.691937	0.813686	0.56916	0.491749	0.194628	0.763884	0.635009	0.425961	0.600227	0.355538	0.096703	0.136706	0.207651	0.277639	0.599995	0.50865	0.299654	142367.9
4	0.114084	0.144439	0.055132	0.720272	0.062027	0.258779	0.353084	0.038602	0.636473	0.85034	0.803429	0.924868	0.806181	0.358857	0.007142	0.50443	0.297825	0.694638	0.448853	0.702866	1930.3
5	0.034541	0.755474	0.851892	0.219441	0.532749	0.382035	0.066466	0.493516	0.647967	0.1401	0.069769	0.103546	0.557345	0.345038	0.621808	0.417813	0.25704	0.858238	0.463051	0.119752	1022543.1
6	0.095174	0.264544	0.763187	0.237975	0.777168	0.759107	0.679167	0.930711	0.025504	0.561014	0.741876	0.167188	0.229481	0.677271	0.090438	0.228749	0.159534	0.498667	0.330174	0.327726	142986.9
7	0.072211	0.405286	0.679865	0.244582	0.655404	0.881224	0.765482	0.387844	0.259324	0.230217	0.631757	0.798782	0.48252	0.690296	0.576038	0.269205	0.564905	0.778981	0.002709	0.362195	435687
8	0.614301	0.030133	0.43868	0.278514	0.940645	0.057301	0.137183	0.288619	0.077186	0.171776	0.079315	0.670364	0.770426	0.3616	0.738607	0.089141	0.1277	0.287163	0.570988	0.260977	1064446.7
9	0.949785	0.726212	0.2906	0.656546	0.320445	0.038351	0.48271	0.425214	0.835405	0.533786	0.526146	0.35036	0.901427	0.128904	0.929766	0.559786	0.550643	0.628759	0.751473	0.029881	184403.7
10	0.536945	0.386602	0.825485	0.759076	0.523664	0.500507	0.333662	0.463655	0.713221	0.710428	0.92543	0.440239	0.301236	0.169734	0.230917	0.823692	0.38991	0.41621	0.138353	0.036424	2130.4
11	0.22587	0.599686	0.789976	0.598144	0.503783	0.202526	0.873167	0.586042	0.934024	0.138624	0.951306	0.980708	0.808283	0.530401	0.896325	0.840313	0.51384	0.832067	0.854344	0.454165	79487.9
12	0.64695	0.897711	0.965634	0.201915	0.297993	0.186404	0.84866	0.559633	0.651441	0.793313	0.8135	0.646678	0.414401	0.408218	0.029729	0.471666	0.855177	0.727191	0.049282	0.272398	16034.6
13	0.005338	0.682572	0.053721	0.776701	0.903579	0.312147	0.77007	0.605628	0.326107	0.619283	0.552992	0.76291	0.51865	0.250861	0.793856	0.316342	0.990211	0.501077	0.309332	0.704286	40082.2
14	0.154811	0.606159	0.99643	0.443671	0.121497	0.135064	0.498195	0.336761	0.585824	0.358976	0.11924	0.082192	0.169138	0.67295	0.040341	0.358252	0.309095	0.395602	0.45065	0.157112	785229.7
15	0.006523	0.371605	0.024329	0.275044	0.981941	0.844997	0.785737	0.4105	0.261254	0.421361	0.514435	0.273033	0.152655	0.894049	0.893089	0.133716	0.352879	0.931411	0.979398	0.725151	559332.2
16	0.035398	0.59838	0.921767	0.798465	0.529747	0.872198	0.110947	0.868952	0.212872	0.085575	0.280361	0.529599	0.534797	0.939852	0.422657	0.908396	0.676884	0.655001	0.590875	0.823192	448831
17	0.181127	0.66959	0.14328	0.929367	0.643068	0.132443	0.954782	0.8321	0.50553	0.687374	0.020436	0.33655	0.28789	0.476686	0.916698	0.864843	0.272412	0.721855	0.312538	0.249966	13375.3
18	0.16759	0.387294	0.450688	0.466438	0.451219	0.781471	0.832622	0.520067	0.412082	0.973701	0.779906	0.00505	0.537775	0.608167	0.295482	0.136452	0.269988	0.639514	0.638172	0.154891	8152.4
19	0.297731	0.951013	0.505903	0.781766	0.116431	0.984011	0.037974	0.560181	0.524662	0.841497	0.130318	0.026851	0.027742	0.179907	0.195185	0.275405	0.340416	0.633955	0.217325	0.041692	250378.3
20	0.910742	0.389507	0.913851	0.731569	0.530669	0.013639	0.526046	0.23999	0.182731	0.536673	0.532311	0.283933	0.135212	0.370857	0.285595	0.802866	0.189796	0.382408	0.256439	0.58473	178938.2
21	0.615935	0.913412	0.208502	0.242087	0.254474	0.659763	0.478573	0.386769	0.740985	0.802727	0.51063	0.872295	0.157521	0.64195	0.098882	0.334707	0.854887	0.444788	0.001647	0.699772	290863.5
22	0.88471	0.577089	0.739674	0.778813	0.495382	0.339487	0.849549	0.685108	0.755225	0.755025	0.077707	0.729292	0.302625	0.220438	0.262007	0.326127	0.559438	0.956624	0.131881	0.474293	81208.4
23	0.991051	0.87196	0.705799	0.942731	0.972844	0.926689	0.961589	0.307812	0.519009	0.763141	0.15985	0.217541	0.483494	0.820264	0.505629	0.829053	0.571262	0.677363	0.128252	0.53163	1312.8

Tabular dataset:

- One label.
- Final cell count.



# Outcomes of virtual drug trials

Drug combination	MYCN_tt	APK_RAS	JAB1_tt	CHK1_tt	ID2_tt	IAP2_tt	HIF_tt	BNIP3_tt	VEGF_tt	p53_tt	p73_tt	p21_tt	p27_tt	cl2_Bclxl	BAK_BAX_t	CAS_tt	CDS1_tt	CDC25C_tt	ALT_tt	telo_tt	Final cell count
1	0.672588	0.512894	0.549193	0.966997	0.730361	0.307462	0.207905	0.292707	0.274859	0.847529	0.95488	0.208644	0.829709	0.314768	0.306795	0.548809	0.512795	0.806082	0.239139	0.057796	2.9
2	0.370603	0.948461	0.176693	0.182967	0.9589	0.166757	0.662312	0.707124	0.517833	0.278251	0.330656	0.703401	0.926063	0.486678	0.728975	0.824148	0.330991	0.479153	0.625507	0.914947	810979.3
3	0.480702	0.361613	0.701094	0.691937	0.813686	0.56916	0.491749	0.194628	0.763884	0.635009	0.425961	0.600227	0.355538	0.096703	0.136706	0.207651	0.277639	0.599995	0.50865	0.299654	142367.9
4	0.114084	0.144439	0.055132	0.720272	0.062027	0.258779	0.353084	0.038602	0.636473	0.85034	0.803429	0.924868	0.806181	0.358857	0.007142	0.50443	0.297825	0.694638	0.448853	0.702866	1930.3
5	0.034541	0.755474	0.851892	0.219441	0.532749	0.382035	0.066466	0.493516	0.647967	0.1401	0.069769	0.103546	0.557345	0.345038	0.621808	0.417813	0.25704	0.858238	0.463051	0.119752	1022543.1
6	0.095174	0.264544	0.763187	0.237975	0.777168	0.759107	0.679167	0.930711	0.025504	0.561014	0.741876	0.167188	0.229481	0.677271	0.090438	0.228749	0.159534	0.498667	0.330174	0.327726	142986.9
7	0.072211	0.405286	0.679865	0.244582	0.655404	0.881224	0.765482	0.387844	0.259324	0.230217	0.631757	0.798782	0.48252	0.690296	0.576038	0.269205	0.564905	0.778981	0.002709	0.362195	435687
8	0.614301	0.030133	0.43868	0.278514	0.940645	0.057301	0.137183	0.288619	0.077186	0.171776	0.079315	0.670364	0.770426	0.3616	0.738607	0.089141	0.1277	0.287163	0.570988	0.260977	1064446.7
9	0.949785	0.726212	0.2906	0.656546	0.320445	0.038351	0.48271	0.425214	0.835405	0.533786	0.526146	0.35036	0.901427	0.128904	0.929766	0.559786	0.550643	0.628759	0.751473	0.029881	184403.7
10	0.536945	0.386602	0.825485	0.759076	0.523664	0.500507	0.333662	0.463655	0.713221	0.710428	0.92543	0.440239	0.301236	0.169734	0.230917	0.823692	0.38991	0.41621	0.138353	0.036424	2130.4
11	0.22587	0.599686	0.789976	0.598144	0.503783	0.202526	0.873167	0.586042	0.974024	0.138624	0.951306	0.980708	0.808283	0.530401	0.896325	0.840313	0.51384	0.832067	0.854344	0.454165	79487.9
12	0.64695	0.897711	0.965634	0.201915	0.297993	0.186404	0.84866	0.559633	0.651441	0.793313	0.8135	0.646678	0.414401	0.408218	0.029729	0.471666	0.855177	0.727191	0.049282	0.272398	16034.6
13	0.005338	0.682572	0.053721	0.776701	0.903579	0.312147	0.77007	0.605628	0.326107	0.619283	0.552992	0.76291	0.51865	0.250861	0.793856	0.316342	0.990211	0.501077	0.309332	0.704286	40082.2
14	0.154811	0.606159	0.99643	0.443671	0.121497	0.135064	0.498195	0.336761	0.585824	0.358976	0.11924	0.082192	0.169138	0.67295	0.040341	0.358252	0.309095	0.395602	0.45065	0.157112	785229.7
15	0.006523	0.371605	0.024329	0.275044	0.981941	0.844997	0.785737	0.4105	0.261254	0.421361	0.514435	0.273033	0.152655	0.894049	0.893089	0.133716	0.352879	0.931411	0.979398	0.725151	559332.2
16	0.035398	0.59838	0.921767	0.798465	0.529747	0.872198	0.110947	0.868952	0.212872	0.085575	0.280361	0.529599	0.534797	0.939852	0.422657	0.908396	0.676884	0.655001	0.590875	0.823192	448831
17	0.181127	0.66959	0.14328	0.929367	0.643068	0.132443	0.954782	0.8321	0.50553	0.687374	0.020436	0.33655	0.28789	0.476686	0.916698	0.864843	0.272412	0.721855	0.312538	0.249966	13375.3
18	0.16759	0.387294	0.450688	0.466438	0.451219	0.781471	0.832622	0.520067	0.412082	0.973701	0.779906	0.00505	0.537775	0.608167	0.295482	0.136452	0.269988	0.639514	0.638172	0.154891	8152.4
19	0.297731	0.951013	0.505903	0.781766	0.116431	0.984011	0.703794	0.560181	0.524662	0.841497	0.130318	0.026851	0.027742	0.179907	0.195185	0.275405	0.340416	0.633955	0.217325	0.041692	250378.3
20	0.910742	0.389507	0.913851	0.731569	0.530669	0.013639	0.526046	0.23999	0.182731	0.536673	0.532311	0.283933	0.135212	0.370857	0.285595	0.802866	0.189796	0.382408	0.256439	0.58473	178938.2
21	0.615935	0.913412	0.208502	0.242087	0.254474	0.659763	0.478573	0.386769	0.740985	0.802727	0.51063	0.872295	0.157521	0.64195	0.098882	0.334707	0.854887	0.444788	0.001647	0.699772	290863.5
22	0.88471	0.577089	0.739674	0.778813	0.495382	0.339487	0.849549	0.685108	0.755225	0.755025	0.077707	0.729292	0.302625	0.220438	0.262007	0.326127	0.559438	0.956624	0.131881	0.474293	81208.4
23	0.991051	0.87196	0.705799	0.942731	0.972844	0.926689	0.961589	0.307812	0.519009	0.763141	0.15985	0.217541	0.483494	0.820264	0.505629	0.829053	0.571262	0.677363	0.128252	0.53163	1312.8

Tabular dataset:

- One label.
- Final cell count.
- 305 effective, **4404 mediocre**, and 291 ineffective combinations.

## Outcomes of virtual drug trials

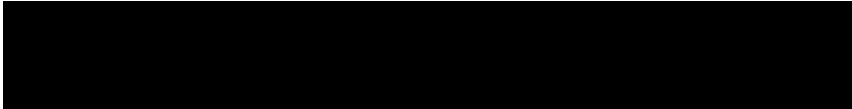
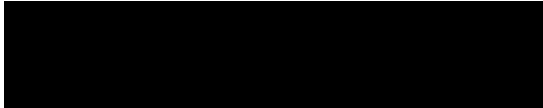
305 effective and 291 ineffective drug combinations. What makes a combination effective?



## Principal component analysis

Direct observables are 20 inhibitory effects. Are there latent variables?

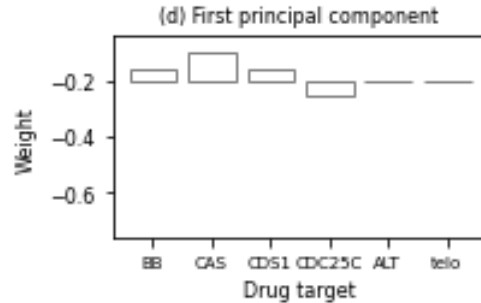
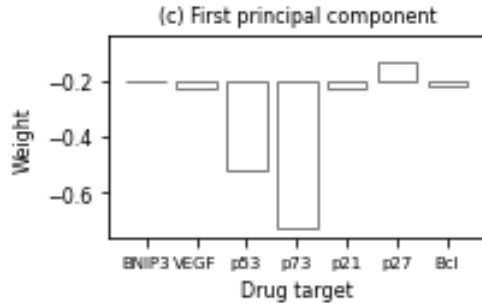
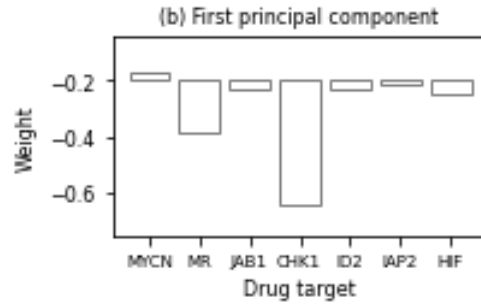
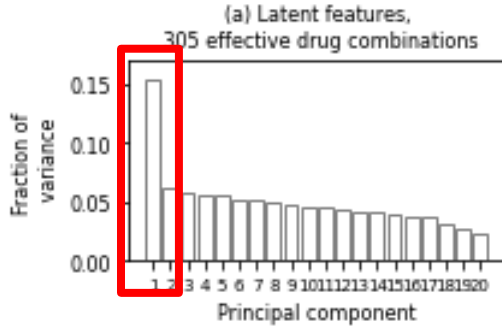
## Connections to Hull University Business School

If the prices of oil, corn, and iron correlate in a dataset, the latent variable is   
.

## Connections to Hull University Business School

If the prices of oil, corn, and iron correlate in a dataset, the latent variable is the general price of commodities.

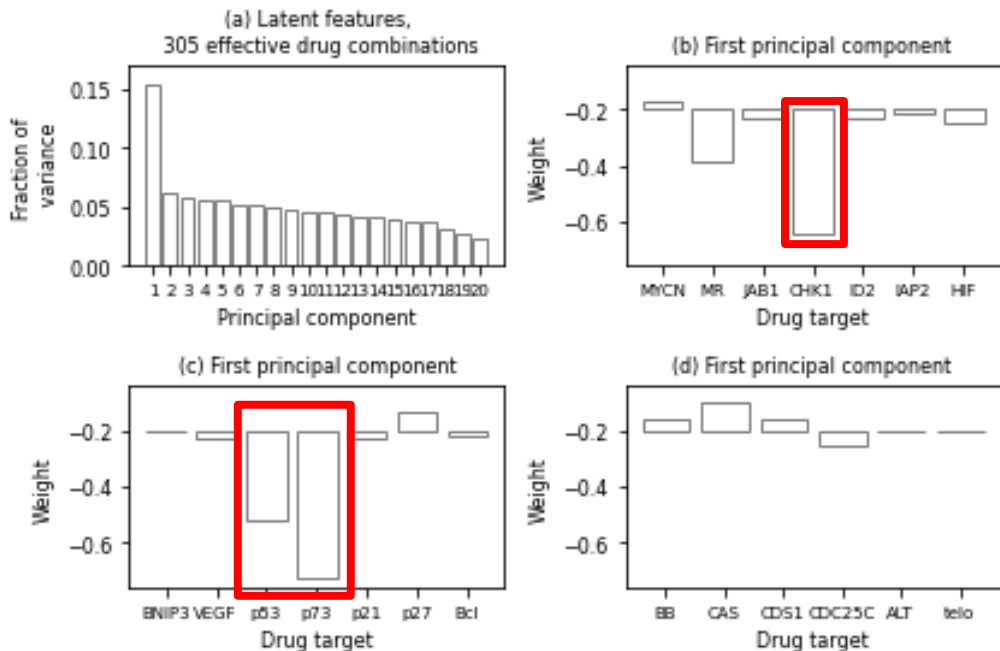
# Principal component analysis



Principal component analysis to identify a latent feature in the 20-dimensional feature space.

Scree plot shows that the first principal component can explain a **substantial amount of variance** in the feature space.

# Principal component analysis



Principal component analysis to identify a latent feature in the 20-dimensional feature space.

Scree plot shows that the first principal component can explain a substantial amount of variance in the feature space.

**Loading plots** show that the latent feature (first principal component) models an inhibitory effect on CHK1, p53, and p73 as a set.

Connections to Hull University Business School

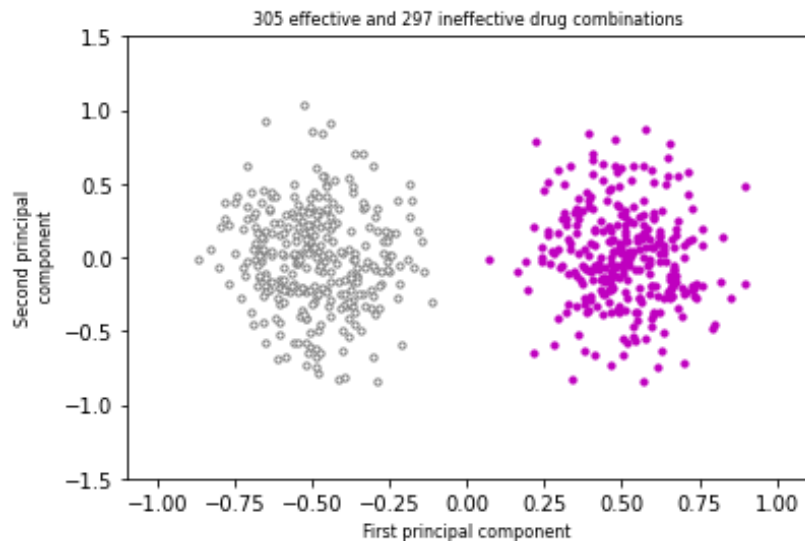
Oil price varies more than iron price  
in the dataset.

# Clustering

Data projected onto and clustered along the first principal component (PC1).

# Clustering

Data projected onto and clustered along the first principal component (PC1).

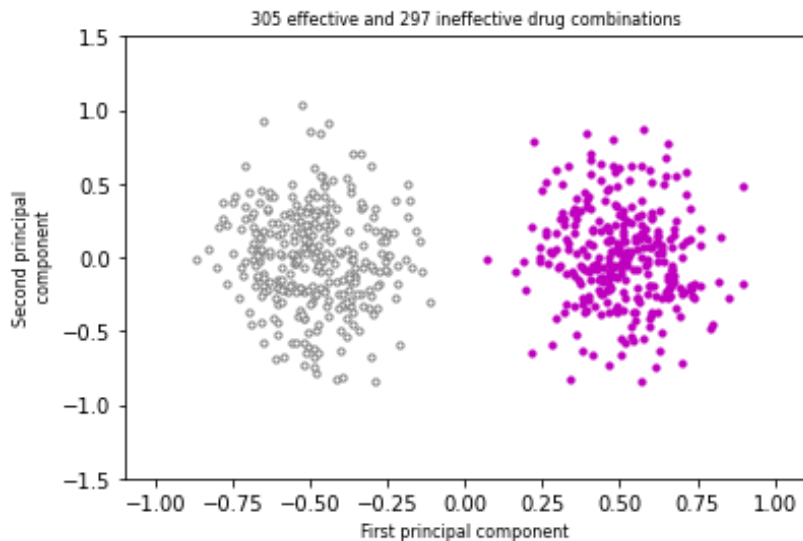


Plotted along the first two principal components: PC1 and PC2.

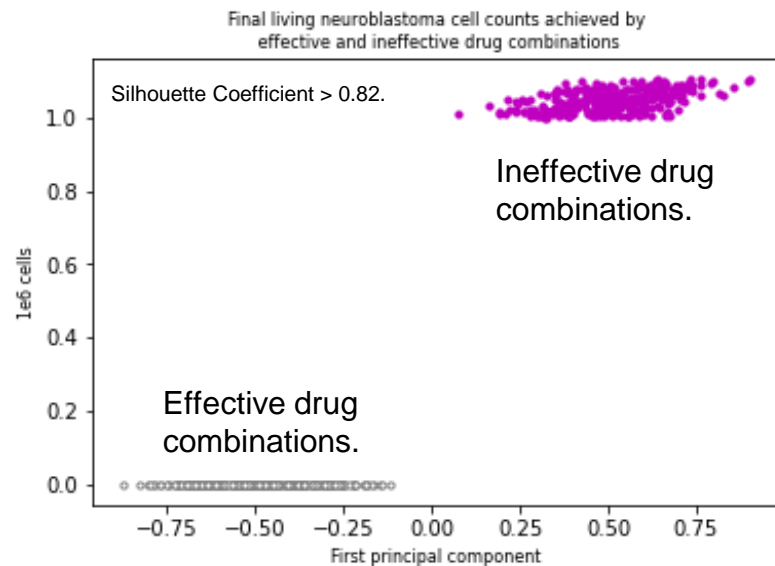


# Clustering

Data projected onto and clustered along the first principal component (PC1).



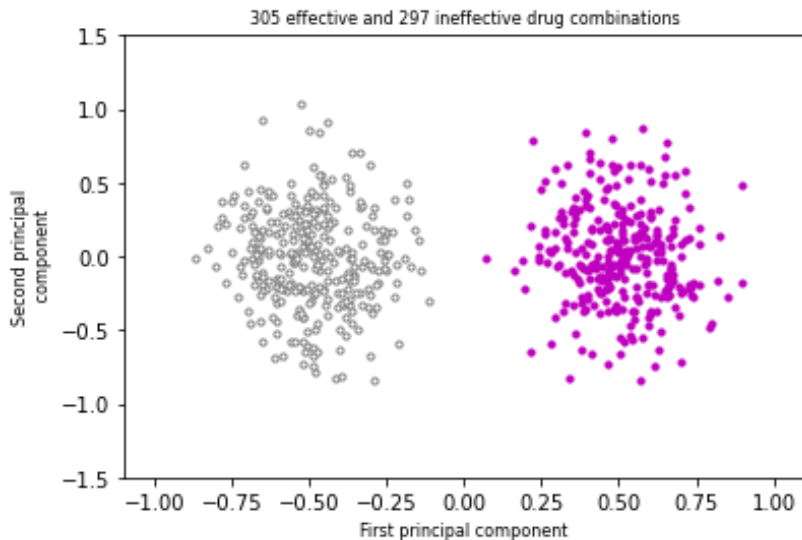
Plotted along the first two principal components: PC1 and PC2.



Comparison of predicted clusters with the labels (effective or ineffective).

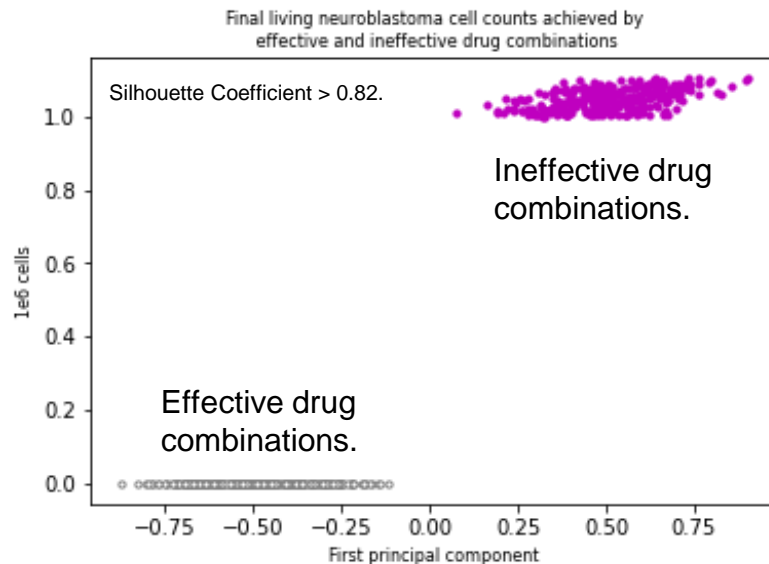
# Clustering

Data projected onto and clustered along the first principal component (PC1).



Plotted along the first two principal components: PC1 and PC2.

Inhibiting CHK1, p53, and p73 together is a winning (or shrinking) strategy.



Comparison of predicted clusters with the labels (effective or ineffective).

# Connections to Hull University Business School



Contents lists available at [ScienceDirect](#)

Technology in Society

journal homepage: <http://www.elsevier.com/locate/techsoc>



Customers segmentation in eco-friendly hotels using multi-criteria and machine learning techniques

Elaheh Yadegaridehkordi<sup>a,\*\*</sup>, Mehrbakhsh Nilashi<sup>b,c,\*</sup>, Mohd Hairul Nizam Bin Md Nasir<sup>d</sup>, Saeedeh Momtazi<sup>e</sup>, Sarminah Samad<sup>f</sup>, Eko Supriyanto<sup>g</sup>, Fahad Ghabban<sup>h</sup>

<sup>a</sup> Information and Communications Technology Research Center, Amirkabir University of Technology, Tehran, Iran

<sup>b</sup> Informatics Research Group, Ton Duc Thang University, Ho Chi Minh City, Viet Nam

<sup>c</sup> Faculty of Information Technology, Ton Duc Thang University, Ho Chi Minh City, Viet Nam

<sup>d</sup> Department of Software Engineering, Faculty of Computer Science & Information Technology, University of Malaya, 50603, Kuala Lumpur, Malaysia

<sup>e</sup> Computer Engineering Department, Amirkabir University of Technology, Tehran, Iran

<sup>f</sup> Department of Business Administration, College of Business and Administration, Princess Nourah Bint Abdulrahman University, Riyadh, Saudi Arabia

<sup>g</sup> School of Biomedical Engineering and Health Sciences, LIN-UTM Cardiovascular Engineering Centre, Faculty of Engineering, Universiti Teknologi Malaysia, Skudai, Johor, 81310, Malaysia

<sup>h</sup> College of Computer Science and Engineering, Information Systems Department, Taibah University, Saudi Arabia

## ARTICLE INFO

### Keywords:

Green hotels  
Decision making  
Segmentation  
Online travel reviews  
Choice behaviour  
Multi-criteria decision making (MCDM)

## ABSTRACT

This study aims to investigate the travellers' choice behaviour towards green hotels through existing online travel reviews on TripAdvisor. Accordingly, a method combining segmentation and the Technique for Order of Preference by Similarity to Ideal Solution (TOPSIS) techniques was developed to segment travellers based on their provided reviews and to prioritize green hotel attributes based on their level of importance in each segment. The data were taken from travellers' online reviews of Malaysian eco-friendly hotels on TripAdvisor. The results showed that the sleep quality was one of the most important factors for eco-hotel selection in the majority of segments. The developed method in this study was able to analyse travellers' reviews and ratings on eco-friendly hotels to identify the future choice behaviour and aid travellers in their decision-making process. The study provides new insights for hotel managers and green policy makers on developing environmental-friendly practices.

## Surrogate modelling

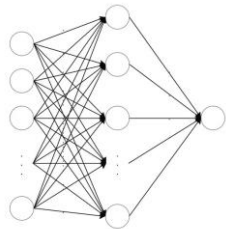
It took around **10 days** to evaluate **5000 drug combinations** on the most advanced GPUs.

# Surrogate modelling

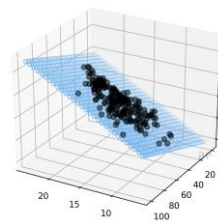
Drug combination	MYCN_tt	APK_RAS	JAB1_tt	CHK1_tt	ID2_tt	IAP2_tt	HIF_tt	BNIP3_tt	VEGF_tt	p53_tt	p73_tt	p21_tt	p27_tt	cl2_Bclxl	AK_BAX_t	CAS_tt	CDS1_tt	CDC25C_tt	ALT_tt	telo_tt	Final cell count
1	0.672588	0.512894	0.549193	0.966997	0.730361	0.307462	0.207905	0.292707	0.274859	0.847529	0.95488	0.208644	0.829709	0.314768	0.306795	0.548809	0.512795	0.806082	0.239139	0.057796	2.9
2	0.370603	0.948461	0.176693	0.182967	0.9589	0.166757	0.662312	0.707124	0.517833	0.278251	0.330656	0.703401	0.926603	0.486678	0.728975	0.824148	0.330991	0.479153	0.625507	0.914947	810979.3
3	0.480702	0.361613	0.701094	0.691937	0.813686	0.56916	0.491749	0.194628	0.763884	0.635009	0.425961	0.600227	0.355538	0.096703	0.136706	0.207651	0.277639	0.599995	0.50865	0.299654	142367.9
4	0.114084	0.144439	0.055132	0.720272	0.062027	0.258779	0.353084	0.038602	0.636473	0.85034	0.803429	0.924868	0.806181	0.358857	0.007142	0.50443	0.297825	0.694638	0.448853	0.702866	1930.3
5	0.034541	0.755474	0.851892	0.219441	0.532749	0.382035	0.066466	0.493516	0.647967	0.1401	0.069769	0.103546	0.557345	0.345038	0.621808	0.417813	0.25704	0.858238	0.463051	0.119752	1022543.1
6	0.095174	0.264544	0.763187	0.237975	0.777168	0.759107	0.679167	0.930711	0.025504	0.561014	0.741876	0.167188	0.229481	0.677271	0.090438	0.228749	0.159534	0.498667	0.330174	0.327726	142986.9
7	0.072211	0.405286	0.679865	0.244582	0.655404	0.881224	0.765482	0.387844	0.259324	0.230217	0.631757	0.798782	0.48252	0.690296	0.576038	0.269205	0.564905	0.778981	0.002709	0.362195	435687
8	0.614301	0.030133	0.43868	0.278514	0.940645	0.057301	0.137183	0.288619	0.077186	0.171776	0.079315	0.670364	0.770426	0.3616	0.738607	0.089141	0.1277	0.287163	0.570988	0.260977	1064446.7
9	0.949785	0.726212	0.2906	0.655646	0.320445	0.038351	0.48271	0.425214	0.835405	0.533786	0.526146	0.35036	0.901427	0.128904	0.929766	0.559786	0.550643	0.628759	0.751473	0.029881	184403.7
10	0.536945	0.386602	0.825485	0.759076	0.523664	0.500507	0.333662	0.463655	0.713221	0.710428	0.92543	0.440239	0.301236	0.169734	0.230917	0.823692	0.38991	0.41621	0.138353	0.036424	2130.4
11	0.22587	0.599686	0.789976	0.598144	0.503783	0.202526	0.873167	0.586042	0.974024	0.138624	0.951306	0.980708	0.808283	0.530401	0.896325	0.840313	0.51384	0.832067	0.854344	0.454165	79487.9
12	0.64695	0.897711	0.965634	0.201915	0.297993	0.186404	0.84866	0.559633	0.651441	0.793313	0.8135	0.646678	0.414401	0.408218	0.029729	0.471666	0.855177	0.727191	0.049282	0.272398	16034.6
13	0.005338	0.682572	0.053721	0.776701	0.903579	0.312147	0.77007	0.605628	0.326107	0.619283	0.552992	0.76291	0.51865	0.250861	0.793856	0.316342	0.990211	0.501077	0.309332	0.704286	40082.2
14	0.154811	0.606159	0.99643	0.443671	0.121497	0.135064	0.498195	0.336761	0.585824	0.358976	0.11924	0.082192	0.169138	0.67295	0.040341	0.358252	0.309095	0.395602	0.45065	0.157112	785229.7
15	0.006523	0.371605	0.024329	0.275044	0.981941	0.844997	0.785737	0.4105	0.261254	0.421361	0.514435	0.273033	0.152655	0.894049	0.893089	0.133716	0.352879	0.931411	0.979398	0.725151	559332.2
16	0.035398	0.59838	0.921767	0.798465	0.529747	0.872198	0.110947	0.868952	0.212872	0.085575	0.280361	0.529599	0.534797	0.939852	0.422657	0.908396	0.676884	0.655001	0.590875	0.823192	448831
17	0.181127	0.66959	0.14328	0.929367	0.643068	0.132443	0.954782	0.8321	0.50553	0.687374	0.020436	0.33655	0.28789	0.476686	0.916698	0.864843	0.272412	0.721855	0.312538	0.249966	13375.3
18	0.16759	0.387294	0.450688	0.466438	0.451219	0.781471	0.832622	0.520067	0.412082	0.973701	0.779906	0.00505	0.537775	0.608167	0.295482	0.136452	0.269988	0.639514	0.638172	0.154891	8152.4
19	0.297731	0.951013	0.505903	0.781766	0.116431	0.984011	0.073974	0.560181	0.524662	0.841497	0.130318	0.026851	0.027742	0.179907	0.195185	0.275405	0.340416	0.633955	0.217325	0.041692	250378.3
20	0.910742	0.389507	0.913851	0.731569	0.530669	0.013639	0.526046	0.23999	0.182731	0.536673	0.532311	0.283933	0.135212	0.370857	0.285595	0.802866	0.189796	0.382408	0.256439	0.58473	178938.2
21	0.615935	0.913412	0.208502	0.242087	0.254474	0.659763	0.478573	0.386769	0.740985	0.802727	0.51063	0.872295	0.157521	0.64195	0.098882	0.334707	0.854887	0.444788	0.001647	0.699772	290863.5
22	0.88471	0.577089	0.739674	0.778813	0.495382	0.339487	0.849549	0.685108	0.755225	0.755025	0.077707	0.729292	0.302625	0.220438	0.262007	0.326127	0.559438	0.956624	0.131881	0.474293	81208.4
23	0.991051	0.87196	0.705799	0.942731	0.972844	0.926689	0.961589	0.307812	0.519009	0.763141	0.15985	0.217541	0.483494	0.820264	0.505629	0.829053	0.571262	0.677363	0.128252	0.53163	1312.8

Tabular dataset:

- 5000 rows/examples.
- 5000 drug combinations.



Multilayer perceptron.



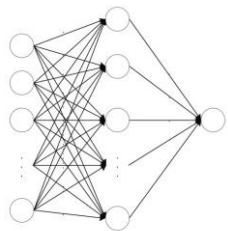
Multiple linear regression.

# Surrogate modelling

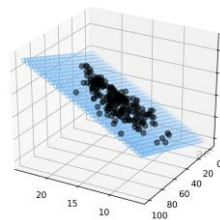
Drug combination	MYCN_tt	APK_RAS	JAB1_tt	CHK1_tt	ID2_tt	IAP2_tt	HIF_tt	BNIP3_tt	VEGF_tt	p53_tt	p73_tt	p21_tt	p27_tt	cl2_Bclxl_t	AK_BAX_t	CAS_tt	CDS1_tt	CDC25C_tt	ALT_tt	telo_tt	Final cell count
1	0.672588	0.512894	0.549193	0.966997	0.730361	0.307462	0.207905	0.292707	0.274859	0.847529	0.95488	0.208644	0.829709	0.314768	0.306795	0.548809	0.512795	0.806082	0.239139	0.057796	2.9
2	0.370603	0.948461	0.176693	0.182967	0.9589	0.166757	0.662312	0.707124	0.517833	0.278251	0.330656	0.703401	0.926063	0.486678	0.728975	0.824148	0.330991	0.479153	0.625507	0.914947	810979.3
3	0.480702	0.361613	0.701094	0.691937	0.813686	0.56916	0.491749	0.194628	0.763884	0.635009	0.425961	0.600227	0.355538	0.096703	0.136706	0.207651	0.277639	0.599995	0.50865	0.299654	142367.9
4	0.114084	0.144439	0.055132	0.720272	0.062027	0.258779	0.353084	0.038602	0.636473	0.85034	0.803429	0.924868	0.806181	0.358857	0.007142	0.50443	0.297825	0.694638	0.448853	0.702866	1930.3
5	0.034541	0.755474	0.851892	0.219441	0.532749	0.382035	0.066466	0.493516	0.647967	0.1401	0.069769	0.103546	0.557345	0.345038	0.621808	0.417813	0.25704	0.858238	0.463051	0.119752	1022543.1
6	0.095174	0.264544	0.763187	0.237975	0.777168	0.759107	0.679167	0.930711	0.025504	0.561014	0.741876	0.167188	0.229481	0.677271	0.090438	0.228749	0.159534	0.498667	0.330174	0.327726	142986.9
7	0.072211	0.405286	0.679865	0.244582	0.655404	0.881224	0.765482	0.387844	0.259324	0.230217	0.631757	0.798782	0.48252	0.690296	0.576038	0.269205	0.564905	0.778981	0.002709	0.362195	435687
8	0.614301	0.030133	0.43868	0.278514	0.940645	0.057301	0.137183	0.288619	0.077186	0.171776	0.079315	0.670364	0.770426	0.3616	0.738607	0.089141	0.1277	0.287163	0.570988	0.260977	1064446.7
9	0.949785	0.726212	0.2906	0.655646	0.320445	0.038351	0.48271	0.425214	0.835405	0.533786	0.526146	0.35036	0.901427	0.128904	0.929766	0.559786	0.550643	0.628759	0.751473	0.029881	184403.7
10	0.536945	0.386602	0.825485	0.759076	0.523664	0.500507	0.333662	0.463655	0.713221	0.710428	0.92543	0.440239	0.301236	0.169734	0.230917	0.823692	0.38991	0.41621	0.138353	0.036424	2130.4
11	0.22587	0.599686	0.789976	0.598144	0.503783	0.202526	0.873167	0.586042	0.974024	0.138624	0.951306	0.980708	0.808283	0.530401	0.896325	0.840313	0.51384	0.832067	0.854344	0.454165	79487.9
12	0.64695	0.897711	0.965634	0.201915	0.297993	0.186404	0.84866	0.559633	0.651441	0.793313	0.8135	0.646678	0.414401	0.408218	0.029729	0.471666	0.855177	0.727191	0.049282	0.272398	16034.6
13	0.005338	0.682572	0.053721	0.776701	0.903579	0.312147	0.77007	0.605628	0.326107	0.619283	0.552992	0.76291	0.51865	0.250861	0.793856	0.316342	0.990211	0.501077	0.309332	0.704286	40082.2
14	0.154811	0.606159	0.99643	0.443671	0.121497	0.135064	0.498195	0.336761	0.585824	0.358976	0.11924	0.082192	0.169138	0.67295	0.040341	0.358252	0.309095	0.395602	0.45065	0.157112	785229.7
15	0.006523	0.371605	0.024329	0.275044	0.981941	0.844997	0.785737	0.4105	0.261254	0.421361	0.514435	0.273033	0.152655	0.894049	0.893089	0.133716	0.352879	0.931411	0.979398	0.725151	559332.2
16	0.035398	0.59838	0.921767	0.798465	0.529747	0.872198	0.110947	0.868952	0.212872	0.085575	0.280361	0.529599	0.534797	0.939852	0.422657	0.908396	0.676884	0.655001	0.590875	0.823192	448831
17	0.181127	0.66959	0.14328	0.929367	0.643068	0.132443	0.954782	0.8321	0.50553	0.687374	0.020436	0.33655	0.28789	0.476686	0.916698	0.864843	0.272412	0.721855	0.312538	0.249966	13375.3
18	0.16759	0.387294	0.450688	0.466438	0.451219	0.781471	0.832622	0.520067	0.412082	0.973701	0.779906	0.00505	0.537775	0.608167	0.295482	0.136452	0.269988	0.639514	0.638172	0.154891	8152.4
19	0.297731	0.951013	0.505903	0.781766	0.116431	0.984011	0.085794	0.560181	0.524662	0.841497	0.130318	0.026851	0.027742	0.179907	0.195185	0.275405	0.340416	0.633955	0.217325	0.041692	250378.3
20	0.910742	0.389507	0.913851	0.731569	0.530669	0.013639	0.526046	0.23999	0.182731	0.536673	0.532311	0.283933	0.135212	0.370857	0.285595	0.802866	0.189796	0.382408	0.256439	0.58473	178938.2
21	0.615935	0.913412	0.208502	0.242087	0.254474	0.659763	0.478573	0.386769	0.740985	0.802727	0.51063	0.872295	0.157521	0.64195	0.098882	0.334707	0.854887	0.444788	0.001647	0.699772	290863.5
22	0.88471	0.577089	0.739674	0.778813	0.495382	0.339487	0.849549	0.685108	0.755225	0.755025	0.077707	0.729292	0.302625	0.220438	0.262007	0.326127	0.559438	0.956624	0.131881	0.474293	81208.4
23	0.991051	0.87196	0.705799	0.942731	0.972844	0.926689	0.961589	0.307812	0.519009	0.763141	0.15985	0.217541	0.483494	0.820264	0.505629	0.829053	0.571262	0.677363	0.128252	0.53163	1312.8

Tabular dataset:

- 5000 rows/examples.
- 5000 drug combinations.



Multilayer perceptron.



Multiple linear regression.

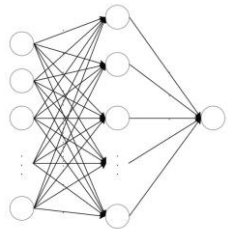


# Surrogate modelling

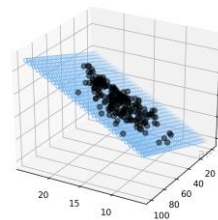
Drug combination	MYCN_tt	APK_RAS	JAB1_tt	CHK1_tt	ID2_tt	IAP2_tt	HIF_tt	BNIP3_tt	VEGF_tt	p53_tt	p73_tt	p21_tt	p27_tt	cl2_Bclxl	AK_BAX_t	CAS_tt	CDS1_tt	CDC25C_tt	ALT_tt	telo_tt	Final count
1	0.672588	0.512894	0.549193	0.966997	0.730361	0.307462	0.207905	0.292707	0.274859	0.847529	0.95488	0.208644	0.829709	0.314768	0.306795	0.548809	0.512795	0.806082	0.239139	0.057796	2.9
2	0.370603	0.948461	0.176693	0.182967	0.9589	0.166757	0.662312	0.707124	0.517833	0.278251	0.330656	0.703401	0.926063	0.486678	0.728975	0.824148	0.330991	0.479153	0.625507	0.914947	810979.3
3	0.480702	0.361613	0.701094	0.691937	0.813686	0.56916	0.491749	0.194628	0.763884	0.635009	0.425961	0.600227	0.355538	0.096703	0.136706	0.207651	0.277639	0.599995	0.50865	0.299654	142367.9
4	0.114084	0.144439	0.055132	0.720272	0.062027	0.258779	0.353084	0.038602	0.636473	0.85034	0.803429	0.924868	0.806181	0.358857	0.007142	0.50443	0.297825	0.694638	0.448853	0.702866	1930.3
5	0.034541	0.755474	0.851892	0.219441	0.532749	0.382035	0.066466	0.493516	0.647967	0.1401	0.069769	0.103546	0.557345	0.345038	0.621808	0.417813	0.25704	0.858238	0.463051	0.119752	1022543.1
6	0.095174	0.264544	0.763187	0.237975	0.777168	0.759107	0.679167	0.930711	0.025504	0.561014	0.741876	0.167188	0.229481	0.677271	0.090438	0.228749	0.159534	0.498667	0.330174	0.327726	142986.9
7	0.072211	0.405286	0.679865	0.244582	0.655404	0.881224	0.765482	0.387844	0.259324	0.230217	0.631757	0.798782	0.48252	0.690296	0.576038	0.269205	0.564905	0.778981	0.002709	0.362195	435687
8	0.614301	0.030133	0.438368	0.278514	0.940645	0.057301	0.137183	0.288619	0.077186	0.171776	0.079315	0.670364	0.770426	0.3616	0.738607	0.089141	0.1277	0.287163	0.570988	0.260977	1064446.7
9	0.949785	0.726212	0.2906	0.655646	0.320445	0.038351	0.48271	0.425214	0.835405	0.533786	0.526146	0.35036	0.901427	0.128904	0.929766	0.559786	0.550643	0.628759	0.751473	0.029881	184403.7
10	0.536945	0.386602	0.825485	0.759076	0.523664	0.500507	0.333662	0.463655	0.713221	0.710428	0.92543	0.440239	0.301236	0.169734	0.230917	0.823692	0.38991	0.41621	0.138353	0.036424	2130.4
11	0.22587	0.599686	0.789976	0.598144	0.503783	0.202526	0.873167	0.586042	0.974024	0.138624	0.951306	0.980708	0.808283	0.530401	0.836325	0.840313	0.51384	0.832067	0.854344	0.454165	79487.9
12	0.64695	0.897711	0.965634	0.201915	0.297993	0.186404	0.84866	0.559633	0.651441	0.793313	0.8135	0.646678	0.414401	0.408218	0.029729	0.471666	0.855177	0.727191	0.049282	0.272398	16034.6
13	0.005338	0.682572	0.053721	0.776701	0.903579	0.312147	0.77007	0.605628	0.326107	0.619283	0.552992	0.76291	0.51865	0.250861	0.793856	0.316342	0.990211	0.501077	0.309332	0.704286	40082.2
14	0.154811	0.606159	0.99643	0.443671	0.121497	0.135064	0.498195	0.336761	0.585824	0.358976	0.11924	0.082192	0.169138	0.67295	0.040341	0.358252	0.309095	0.395602	0.45065	0.157112	785229.7
15	0.006523	0.371605	0.024329	0.275044	0.981941	0.844997	0.785737	0.4105	0.261254	0.421361	0.514435	0.273033	0.152655	0.894049	0.893089	0.133716	0.352879	0.931411	0.979398	0.725151	559332.2
16	0.035398	0.59838	0.921767	0.798465	0.529747	0.872198	0.110947	0.868952	0.212872	0.085575	0.280361	0.529599	0.534797	0.939852	0.422657	0.908396	0.676884	0.655001	0.590875	0.823192	448831
17	0.181127	0.66959	0.14328	0.929367	0.643068	0.132443	0.954782	0.8321	0.50553	0.687374	0.020436	0.33655	0.28789	0.476686	0.916698	0.864843	0.272412	0.721855	0.312538	0.249966	13375.3
18	0.16759	0.387294	0.450688	0.466438	0.451219	0.781471	0.832622	0.520067	0.412082	0.973701	0.779906	0.00505	0.537775	0.608167	0.295482	0.136452	0.269988	0.639514	0.638172	0.154891	8152.4
19	0.297731	0.951013	0.505903	0.781766	0.116431	0.984011	0.087394	0.560811	0.524662	0.841497	0.130318	0.026851	0.027742	0.179907	0.195185	0.275405	0.340416	0.633955	0.217325	0.041692	250378.3
20	0.910742	0.389507	0.913851	0.731569	0.530669	0.013639	0.526046	0.23999	0.182731	0.536673	0.532311	0.283933	0.135212	0.370857	0.285595	0.802866	0.189796	0.382408	0.256439	0.58473	178938.2
21	0.615935	0.913412	0.208502	0.242087	0.254474	0.659763	0.478573	0.386769	0.740985	0.802727	0.51063	0.872295	0.157521	0.64195	0.098882	0.334707	0.854887	0.444788	0.001647	0.699772	290863.5
22	0.88471	0.577089	0.739674	0.778813	0.495382	0.339487	0.849549	0.685108	0.755225	0.755025	0.077707	0.729292	0.302625	0.220438	0.262007	0.326127	0.559438	0.956624	0.131881	0.474293	81208.4
23	0.991051	0.87196	0.705799	0.942731	0.972844	0.962689	0.961589	0.307812	0.519009	0.763141	0.15985	0.217541	0.483494	0.820264	0.505629	0.829053	0.571262	0.677363	0.128252	0.53163	1312.8

Tabular dataset:

- 5000 rows/examples.
- 5000 drug combinations.



Multilayer perceptron.



Multiple linear regression.

## Surrogate modelling

It took around 10 days to evaluate 5000 drug combinations on the most advanced GPUs.

A **deep learning model** could hypothetically evaluate **several million combinations in a few hours.**



**Get more out of a dataset by extrapolation!**



# Connections to Hull University Business School

JOURNAL OF PROPERTY RESEARCH  
2021, VOL. 38, NO. 1, 48–70  
<https://doi.org/10.1080/09599916.2020.1832558>



 OPEN ACCESS  Check for updates

## Predicting property prices with machine learning algorithms

Winky K.O. Ho<sup>a</sup>, Bo-Sin Tang<sup>b</sup> and Siu Wai Wong<sup>c</sup>

<sup>a</sup>Department of Real Estate and Construction, The University of Hong Kong, Hong Kong, China; <sup>b</sup>Department of Urban Planning and Design, The University of Hong Kong, Hong Kong, China; <sup>c</sup>Department of Building and Real Estate, The Hong Kong Polytechnic University, Hong Kong, China

### ABSTRACT

This study uses three machine learning algorithms including, support vector machine (SVM), random forest (RF) and gradient boosting machine (GBM) in the appraisal of property prices. It applies these methods to examine a data sample of about 40,000 housing transactions in a period of over 18 years in Hong Kong, and then compares the results of these algorithms. In terms of predictive power, RF and GBM have achieved better performance when compared to SVM. The three performance metrics including mean squared error (MSE), root mean squared error (RMSE) and mean absolute percentage error (MAPE) associated with these two algorithms also unambiguously outperform those of SVM. However, our study has found that SVM is still a useful algorithm in data fitting because it can produce reasonably accurate predictions within a tight time constraint. Our conclusion is that machine learning offers a promising, alternative technique in property valuation and appraisal research especially in relation to property price prediction.

### ARTICLE HISTORY

Received 27 February 2020  
Accepted 1 October 2020

### KEYWORDS

Machine Learning  
algorithms; SVM; RF; GBM;  
property valuation

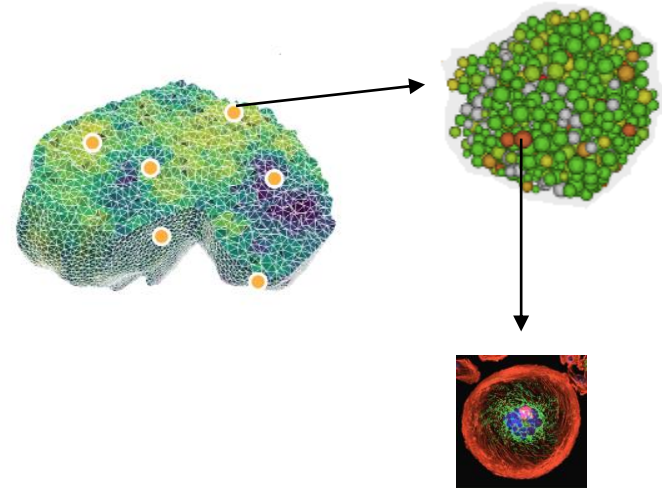
Ho, Winky KO, Bo-Sin Tang, and Siu Wai Wong. "Predicting property prices with machine learning algorithms." *Journal of Property Research* 38.1 (2021): 48-70.

# Lecture outline

- ~~1. Neuroblastoma.~~
- ~~2. Multiscale problem.~~
- ~~3. Tumour scale.~~
- ~~4. Tissue scale.~~
- 5. Cellular scale.**

Inside an individual

Scale: One cancer cell.

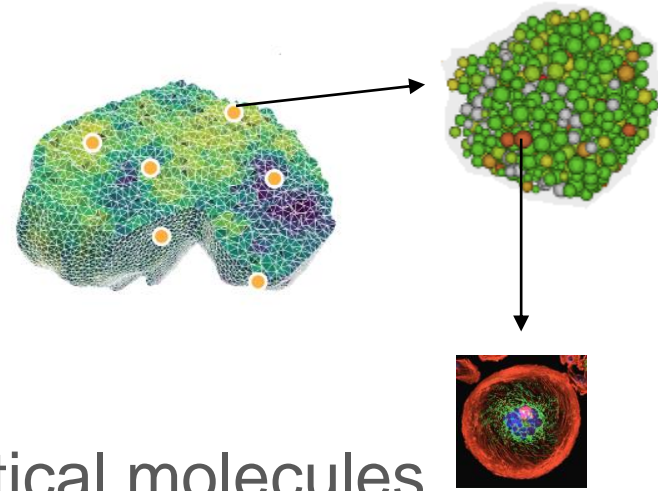


Inside an individual

Scale: One cancer cell.

Resolution: Population containing identical molecules.

A cell is represented by the intracellular concentrations of selected molecular species.



Inside an individual

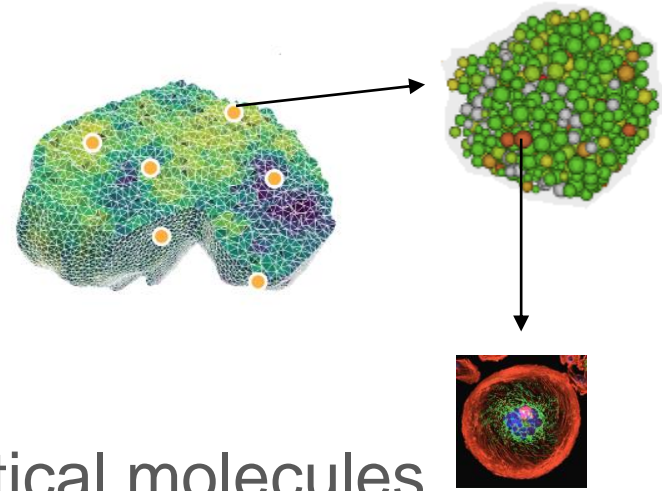
Scale: One cancer cell.

Resolution: Population containing identical molecules.

A cell is represented by the intracellular concentrations of selected molecular species.

Modelling framework: Differential equations.

Like population-based approach  
at the tumour scale.

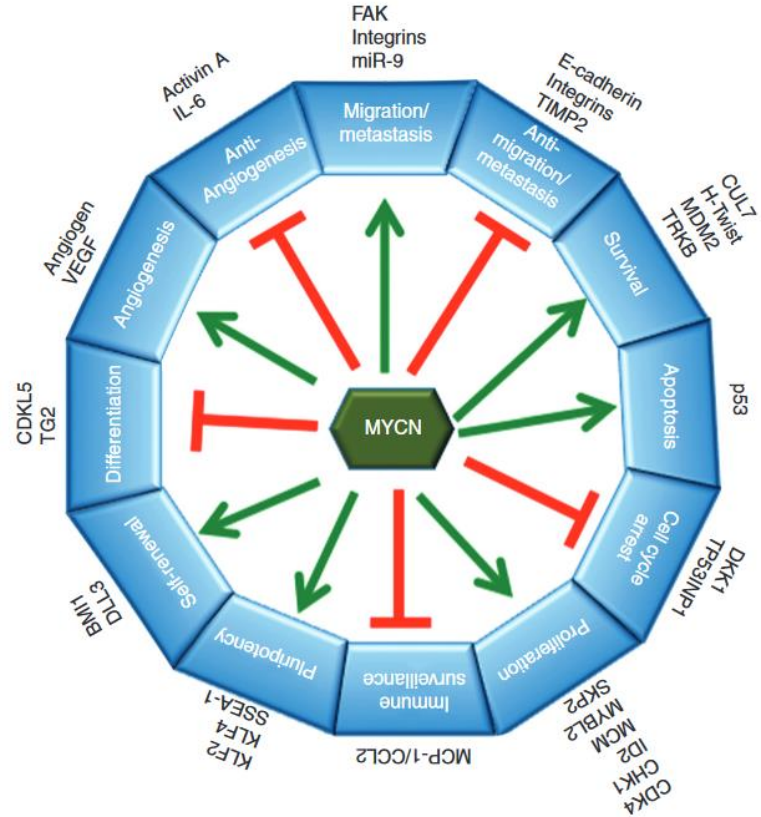


# MYCN enigma

Oncogene.

Multiple roles in malignancy and maintenance of stem-like state.

Disease outcome should get worse monotonically as MYCN expression level goes up.



Huang, Miller, and William A. Weiss. "Neuroblastoma and MYCN." *Cold Spring Harbor perspectives in medicine* 3.10 (2013): a014415.

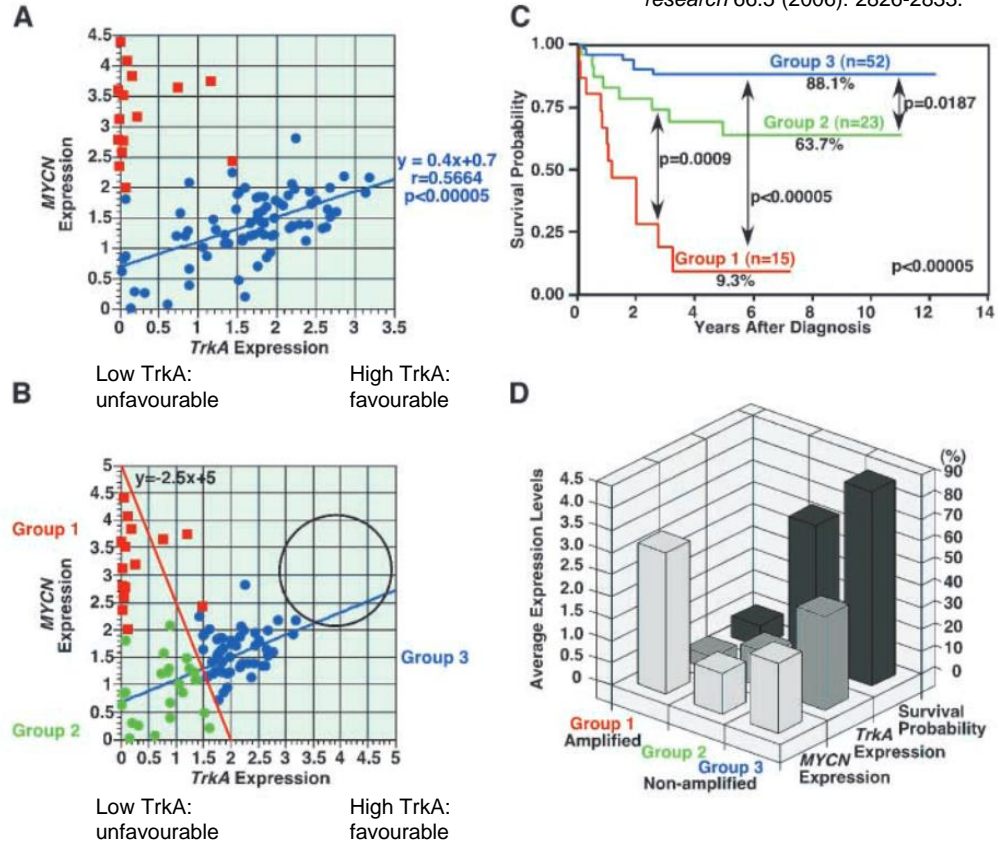
# MYCN enigma

‘This **nonlinear distribution of disease outcome relative to MYCN expression in neuroblastoma** explains why MYCN expression is not predictive of neuroblastoma disease outcome by dichotomous division of the neuroblastoma cohort.’

Expectation: MYCN up, outcome gets worse.

Reality: MYCN up, outcome gets better before getting worse.

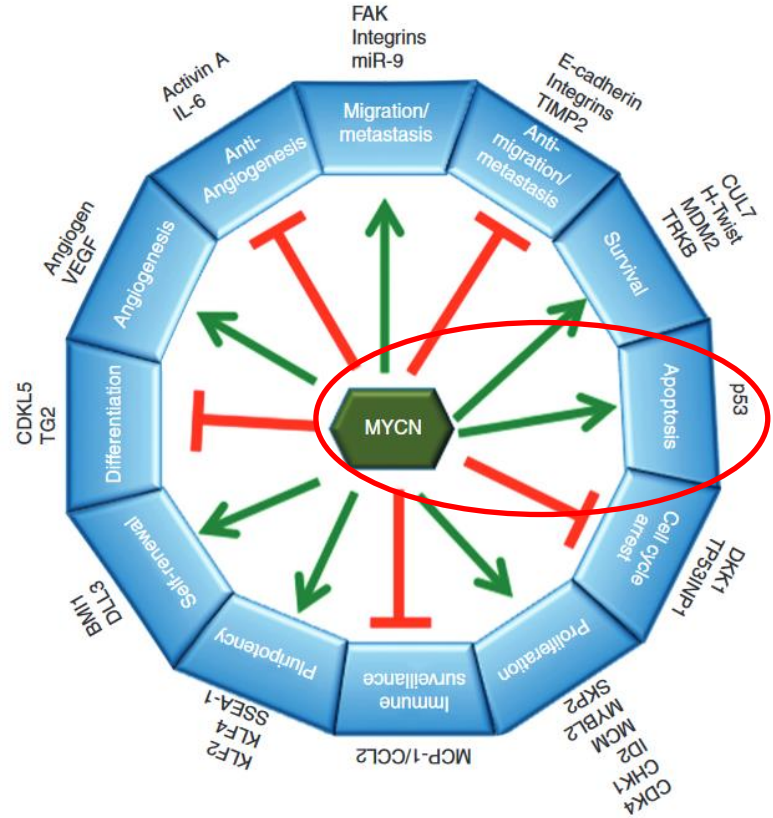
Tang, Xiao X., et al. "The MYCN enigma: significance of MYCN expression in neuroblastoma." *Cancer research* 66.5 (2006): 2826-2833.



# Hypothesis

MYCN is an oncogene.

MYCN also upregulates p53, a tumour suppressor gene.



Huang, Miller, and William A. Weiss. "Neuroblastoma and MYCN." *Cold Spring Harbor perspectives in medicine* 3.10 (2013): a014415.

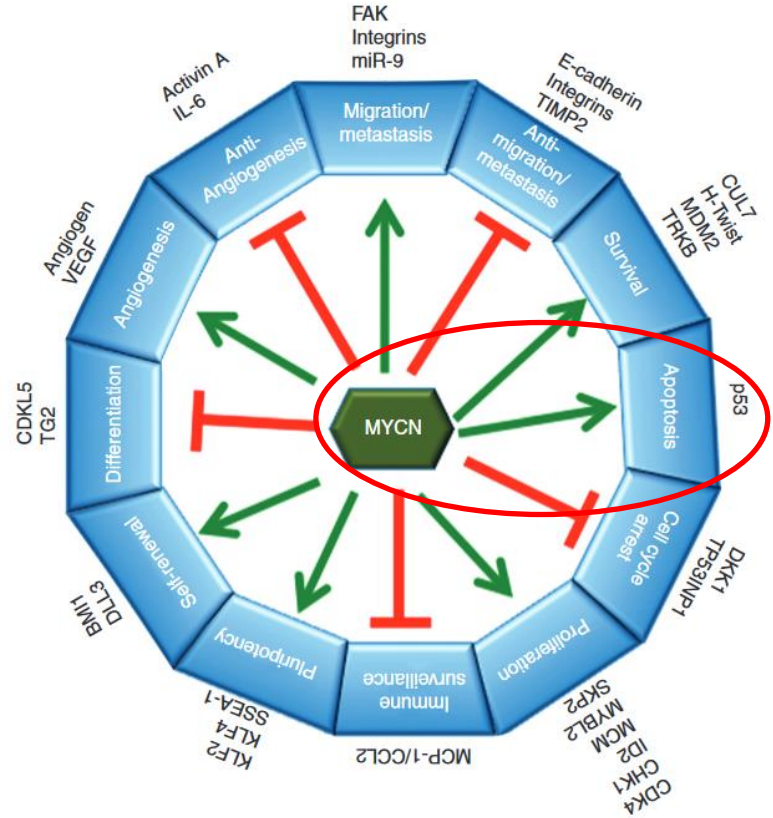


# Hypothesis

MYCN is an oncogene.

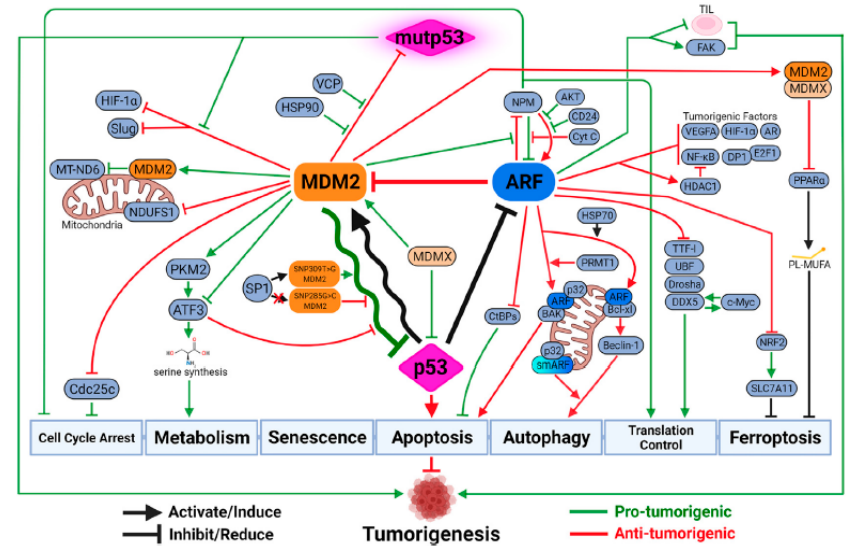
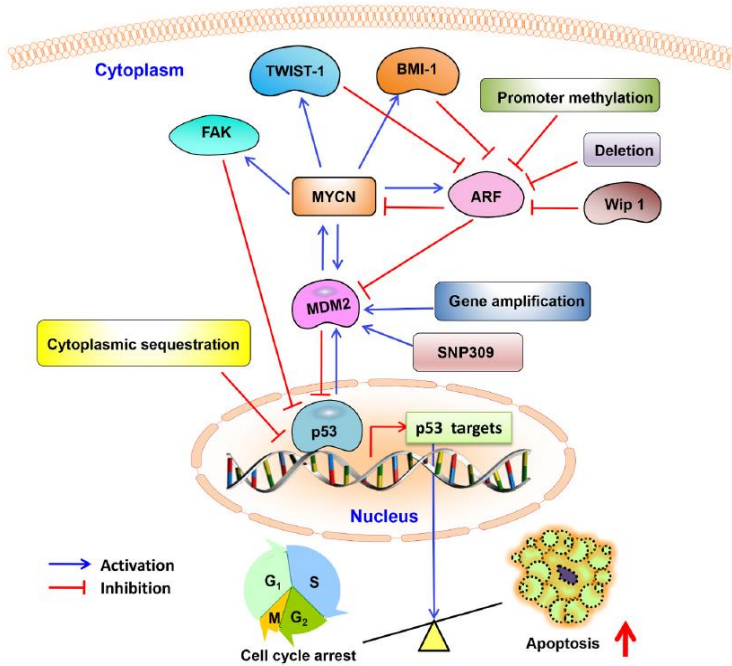
MYCN also upregulates p53, a tumour suppressor gene.

Disease outcome should get worse monotonically as p53/MYCN level goes down.



Huang, Miller, and William A. Weiss. "Neuroblastoma and MYCN." *Cold Spring Harbor perspectives in medicine* 3.10 (2013): a014415.

# Molecular context

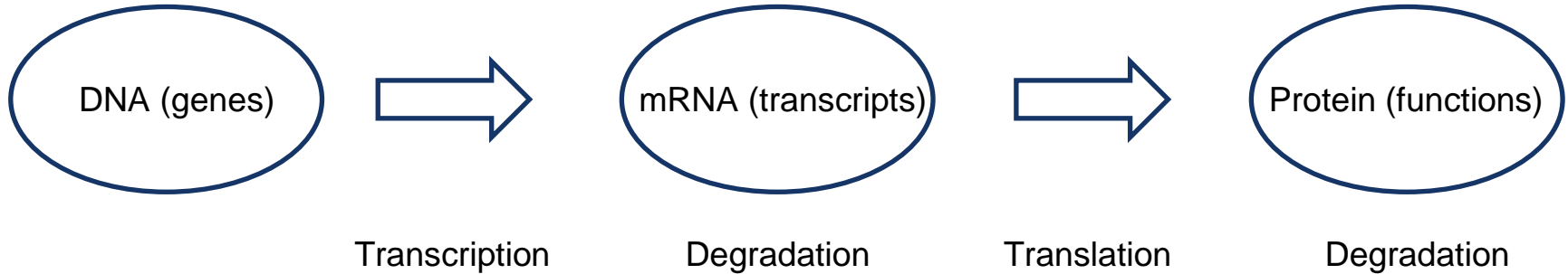


Kung, Che-Pei, and Jason D. Weber. "It's getting complicated—a fresh look at p53-MDM2-ARF triangle in tumorigenesis and cancer therapy." *Frontiers in cell and developmental biology* 10 (2022): 818744.

MYCN, p53, ARF, and MDM2 form a gene regulatory network.

Four pairs of equations.

# Central dogma of molecular biology



$$\frac{d}{dt}[m_i(t)] = k_i - \delta_{m_i}[m_i(t)]$$

Rate of change of  
mRNA level.

$$\frac{d}{dt}[p_i(t)] = l_i[m_i(t)] - \delta_{p_i}[p_i(t)]$$

Rate of change of  
protein level.

# Model structure

$$\frac{d}{dt}[MYCN_m] = g_{MYCN} \left\{ \phi_{MYCN} \alpha_{MYCN} + (1 - \phi_{MYCN}) \beta_{MYCN} \right\} - \left\{ \varphi_{MYCN} d_{MYCN_m} + (1 - \varphi_{MYCN}) d_{MYCN_m-G} \right\} [MYCN_m].$$

$$\frac{d}{dt}[MYCN] = \left\{ \sigma_{MYCN} \lambda_{MYCN} + (1 - \sigma_{MYCN}) \mu_{MYCN} \right\} [MYCN_m] - \left\{ \theta_{MYCN} d_{MYCN} + (1 - \theta_{MYCN}) d_{MYCN-A} \right\} [MYCN].$$

$$\frac{d}{dt}[P53_m] = g_{P53} \left\{ \phi_{P53} \alpha_{P53} + (1 - \phi_{P53}) \beta_{P53} \right\} - d_{P53_m} [P53_m].$$

$$\begin{aligned} \frac{d}{dt}[P53] = & \sigma_{P53} \left\{ \lambda_{P53} + \frac{\kappa_{P53}(\theta_{MDM2}[MDM2])(1 - Ss_2)}{K_9} \right. \\ & \left. + \frac{\mu_{P53}(\theta_{MDM2}[MDM2])(Ss_2)}{K_{10}} \right\} [P53_m] \\ & - \theta_{P53} \left\{ d_{P53} + \left( \frac{(1 - s_3)S}{K_C} d_{P53-C} + \frac{(1 - s_4)S}{K_D} d_{P53-D} \right) [MDM2] \right. \\ & \left. + \frac{(1 - s_4)S}{K_F} d_{P53-F} [ARF][MDM2] \right\} [P53]. \end{aligned}$$

$$\frac{d}{dt}[MDM2_m] = g_{MDM2} \left\{ \phi_{MDM2} \alpha_{MDM2} + (1 - \phi_{MDM2}) \beta_{MDM2} \right\} - d_{MDM2_m} [MDM2_m].$$

$$\begin{aligned} \frac{d}{dt}[MDM2] = & \lambda_{MDM2} [MDM2_m] \\ & - \theta_{MDM2} \left\{ d_{MDM2} + \frac{d_{MDM2-B}}{K_B} [ARF] \right. \\ & + \left( \frac{(1 - s_3)S}{K_C} d_{MDM2-C} + \frac{(1 - s_4)S}{K_D} d_{MDM2-D} \right) [P53] \\ & + \frac{s_5 S}{K_E} d_{MDM2-E} [MDM2] \\ & \left. + \frac{(1 - s_4)S}{K_F} d_{MDM2-F} [P53][ARF] \right\} [MDM2]. \end{aligned}$$

$$\frac{d}{dt}[ARF_m] = g_{ARF} \phi_{ARF} \left( \alpha_{ARF} + \frac{\beta_{ARF} (s_1 S)^{h_6}}{K_6^{h_6}} \right) - d_{ARF_m} [ARF_m].$$

$$\begin{aligned} \frac{d}{dt}[ARF] = & \lambda_{ARF} [ARF_m] \\ & - (1 - s_6 S) \theta_{ARF} \left\{ d_{ARF} + \frac{d_{ARF-A}}{K_A} [MYCN] + \frac{d_{ARF-B}}{K_B} [MDM2] \right. \\ & \left. + \frac{(1 - s_4)S}{K_F} d_{ARF-F} [P53][MDM2] \right\} [ARF]. \end{aligned}$$

# Model structure

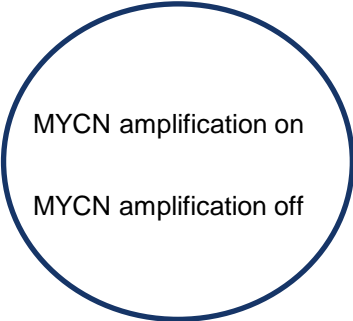
$\phi_{MYCN}$	$\frac{1}{1 + \frac{M_1^{h_1}}{K_1^{h_1}}}$
$\phi_{P53}$	$\frac{1}{1 + \frac{\theta_{MYCN}[MYCN]}{K_2} + \frac{(\theta_{P53}[P53])^{1.8}}{K_3^{1.8}} + \frac{\theta_{MYCN}[MYCN](\theta_{P53}[P53])^{1.8}}{K_2 K_3^{1.8}}}$
$\phi_{MDM2}$	$\frac{1}{1 + \frac{\theta_{MYCN}[MYCN]}{K_4} + \frac{(\theta_{P53}[P53])^{1.8}}{K_5^{1.8}} + \frac{\theta_{MYCN}[MYCN](\theta_{P53}[P53])^{1.8}}{K_4 K_5^{1.8}}}$
$\phi_{ARF}$	$\frac{1}{1 + \frac{(s_1 S)^{h_6}}{K_6^{h_6}} + \frac{(\theta_{P53}[P53])^{1.8}}{K_7^{1.8}} + \frac{(s_1 S)^{h_6} (\theta_{P53}[P53])^{1.8}}{K_6^{h_6} K_7^{1.8}}}$

$\varphi_{MYCN}$	$\frac{1 + \frac{M_2^{h_8}}{K_8^{h_8}}}{1 + \frac{\theta_{MDM2}[MDM2]}{K_G} + \frac{M_2^{h_8}}{K_8^{h_8}} + \frac{\theta_{MDM2}[MDM2]M_2^{h_8}}{K_G K_8^{h_8}}}$
------------------	--

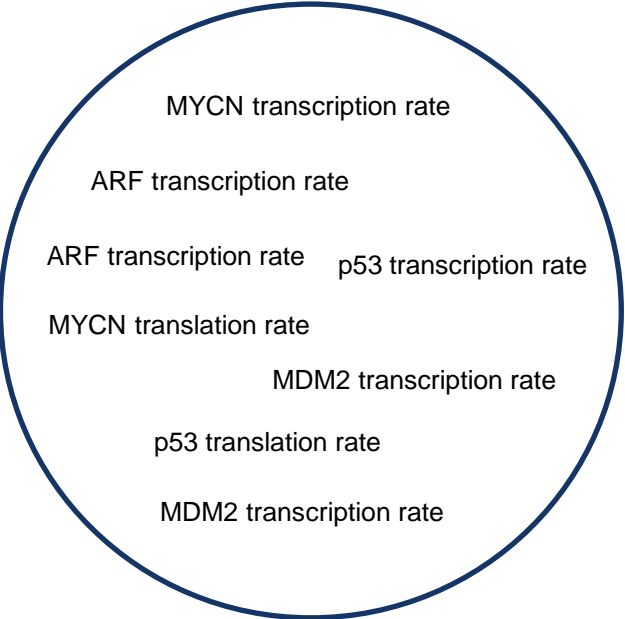
$\sigma_{MYCN}$	$\frac{1 + \frac{\theta_{MDM2}[MDM2]}{K_G}}{1 + \frac{\theta_{MDM2}[MDM2]}{K_G} + \frac{M_2^{h_8}}{K_8^{h_8}} + \frac{\theta_{MDM2}[MDM2]M_2^{h_8}}{K_G K_8^{h_8}}}$
$\sigma_{P53}$	$\frac{1}{1 + \frac{(\theta_{MDM2}[MDM2])(1-s_2 S)}{K_9} + \frac{(\theta_{MDM2}[MDM2])(s_2 S)}{K_{10}}}$
$\theta_{MYCN}$	$\frac{1}{1 + \frac{[ARF]}{K_A}}$
$\theta_{P53}$	$\frac{1}{1 + \left( \frac{(1-s_3 S)}{K_C} + \frac{(1-s_4 S)}{K_D} \right) [MDM2] + \frac{(1-s_4 S)[MDM2][ARF]}{K_F}}$
$\theta_{MDM2}$	$\frac{1}{1 + \frac{[ARF]}{K_B} + \left( \frac{(1-s_3 S)}{K_C} + \frac{(1-s_4 S)}{K_D} \right) [P53] + \frac{s_5 S[MDM2]}{K_E} + \frac{(1-s_4 S)[ARF][P53]}{K_F}}$
$\theta_{ARF}$	$\frac{1}{1 + \frac{[MYCN]}{K_A} + \frac{[MDM2]}{K_B} + \frac{(1-s_4 S)[MDM2][P53]}{K_F}}$

# Simulations

High, medium, and low.

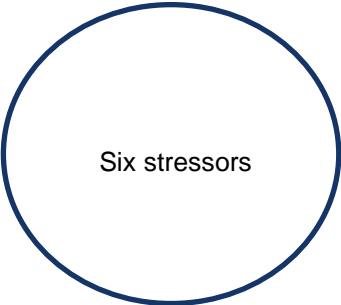


Two possibilities.



$3^8=6561$  possibilities.

On or off.



$2^6=64$  possibilities.

# Simulations

Exploration of parametric space.  
Almost one million points there.

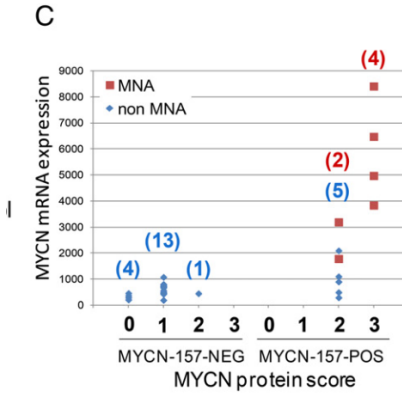
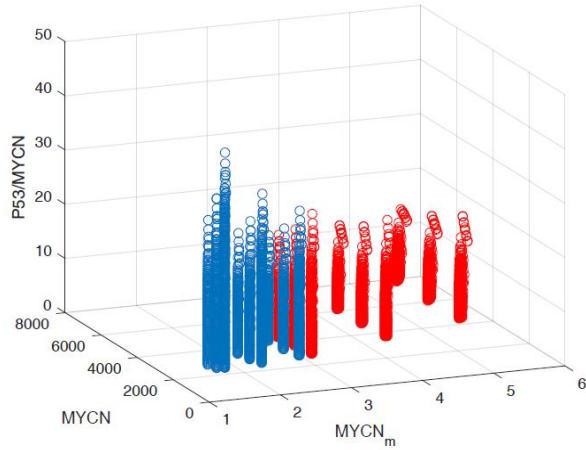
# Simulations

Hypothesis: Disease outcome should get worse monotonically as p53/MYCN (protein levels) goes down.

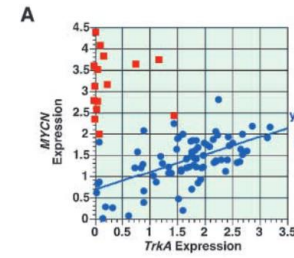
Each parametric combination, ran a simulation, classified the outcome based on p53/MYCN (protein levels) and MYCN amplification status.



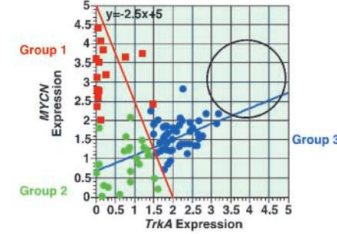
# Simulation results



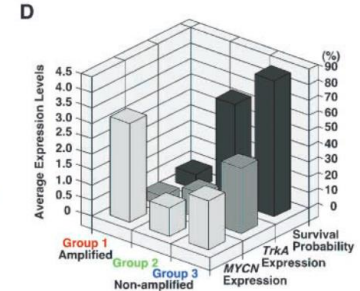
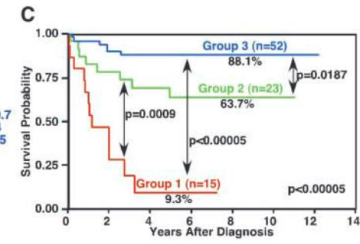
Valentijn, Linda J., et al. "Functional MYCN signature predicts outcome of neuroblastoma irrespective of MYCN amplification." *Proceedings of the National Academy of Sciences* 109.47 (2012): 19190-19195.



Low TrkA: unfavourable      High TrkA: favourable



Low TrkA: unfavourable      High TrkA: favourable

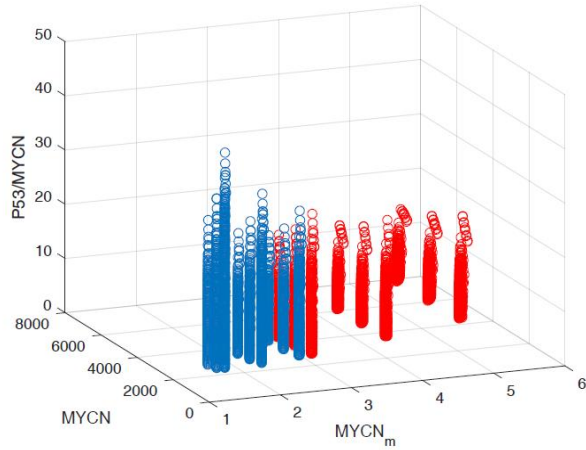


Tang, Xiao X., et al. "The MYCN enigma: significance of MYCN expression in neuroblastoma." *Cancer research* 66.5 (2006): 2826-2833.

Interpreted through the lens of the hypothesis, simulation results agree with clinical data (MYCN enigma).

Hypothesis can explain the MYCN enigma!

# Simulation results



	High p53/MYCN (good)	Low p53/MYCN (bad)
MYCN amplified	134,495 cases	285,409 cases
MYCN not amplified	317,699 cases	102,205 cases

Four baskets of parametric combinations.

Used Apriori algorithm to find patterns (association rules) in each basket.

# Simulation results



	High p53/MYCN (good)	Low p53/MYCN (bad)
MYCN amplified	134,495 cases	285,409 cases
MYCN not amplified	317,699 cases	102,205 cases

Four baskets of parametric combinations.

Used Apriori algorithm to find patterns (association rules) in each basket.

# Simulation results



	High p53/MYCN (good)	Low p53/MYCN (bad)
MYCN amplified	134,495 cases	285,409 cases
MYCN not amplified	317,699 cases	102,205 cases

In a bad case (poor clinical outcome), one and only one of p53's transcription and translation rates is high.

Conjecture: p53 transcription and translation depend on a common limiting species controlled by p53 (positively) and MYCN (negatively).

# Connections to Hull University Business School

## A Recommendation Model Based on User Behaviors on Commercial Websites Using TF-IDF, KMeans, and Apriori Algorithms

[Piyanuch Chaipornkaew](#)  & [Thepparit Banditwattanawong](#)

Conference paper | First Online: 25 June 2021

369 Accesses | 5 Citations

Part of the book series: [Lecture Notes in Networks and Systems](#) ((LNNS, volume 251))

### Abstract

---

In recent years, recommendation systems have been widely introduced in various domains. The three main types of recommendation system are content-based, collaborative and hybrid filtering. Nowadays, much research applies machine learning techniques to construct recommendation models. This research also implemented a recommendation model using three machine learning techniques: TF-IDF, KMeans, and Apriori algorithms. TF-IDF was applied to form word vectorization from webpage headings. KMeans was utilized for clustering webpage headings while the Apriori algorithm was employed to find the association of webpage clusters. The elbow method was utilized to obtain the optimal number of clusters. KNN, Decision Tree, and Multi-Layer Perceptron were employed to evaluate the prediction accuracy. The dataset analyzed in the research was collected from a specific commercial website. User behaviors on the website were considered as the dataset in the research. The recommendation lists were retrieved from webpages in the same cluster and associated clusters. The prediction accuracy of the proposed model was approximately 88.62%.

Chaipornkaew, Piyanuch, and Thepparit Banditwattanawong. "A recommendation model based on user behaviors on commercial websites using TF-IDF, KMeans, and Apriori algorithms." *International Conference on Computing and Information Technology*. Cham: Springer International Publishing, 2021.

# Lecture outline

- ~~1. Neuroblastoma.~~
- ~~2. Multiscale problem.~~
- ~~3. Tumour scale.~~
- ~~4. Tissue scale.~~
- ~~5. Cellular scale.~~

# Summary

- Cancer research requires a systemic approach.
- Different scales require different modelling frameworks.
- Mathematical modelling, scientific computing, and machine learning synergise.
- DAIM and Hull University Business School can learn from each other.
- Let's apply for grants together.